

ENHANCING CORTICOSPINAL TRACT NEURITE OUTGROWTH
USING HISTONE DEACETYLASE INHIBITORS

by

CHRISTIE MCSHANE

HBSc. The University of Toronto, 2005

A THESIS SUBMITTED IN PARTIAL FULFILLMENT OF
THE REQUIREMENTS FOR THE DEGREE OF

MASTER OF SCIENCE

in

THE FACULTY OF GRADUATE STUDIES

(Cellular and Developmental Sciences)

THE UNIVERSITY OF BRITISH COLUMBIA

(Vancouver)

July 2011

© Christie McShane, 2011

ABSTRACT

The human corticospinal tract (CST) is responsible for coordinated voluntary movement and it contains descending afferent inputs involved in autonomic control and gating of spinal reflexes. After spinal cord injury (SCI), damage to the CST causes degeneration of axons and can result in major motor impairments. The CST is especially lacking in its capacity to regenerate after injury. In the current study, we harvested the cortices of postnatal day 8 Thy1YFP16JRS mice, which express YFP in layer five projection neurons, which also express CST transcription factors *Ctip2* and *Otx1* *in vitro*. We applied Histone deacetylase (HDAC) inhibitors (Trichostatin A [TSA] and Tubastatin A) to the mixed neuron culture and assessed survival and neurite outgrowth of YFP positive CST neurons. TSA treatment increased the number of primary neurites per neuron and the number of branch points exhibited by YFP positive CST neurons. Application of either TSA or Tubastatin A, promoted YFP positive CST neurite outgrowth in baseline media as well as in the presence of the neurotrophin 3 (NT3) and ciliary neurotrophic factor (CNTF), compared to the appropriate controls. Taken together, the application of HDAC inhibitors to postnatal corticospinal neurons can promote neurite outgrowth, branching and an increase in the number of primary neurites when grown in baseline media.

PREFACE

All studies were performed under the approval and guidelines of the Canadian Council for Animal Care, and the Animal Care Committee of the University of British Columbia (animal approval number A07-0279).

TABLE OF CONTENTS

ABSTRACT	ii
PREFACE	iii
LIST OF TABLES	vi
LIST OF FIGURES	vii
LIST OF ABBREVIATIONS	ix
ACKNOWLEDGEMENTS	xi
CHAPTER 1 : INTRODUCTION	1
1.1 Corticospinal Tract Neurons: Function, Development and Injury	1
1.2 Spinal Cord Injury: Barriers to Regeneration and Therapeutic Strategies	5
1.2.1 <i>Bridging the lesion gap with cell therapies</i>	5
1.2.2 <i>Neurotrophic support</i>	8
1.2.3 <i>Neutralizing the inhibitory lesion environment</i>	9
1.2.3.1 <i>Myelin associated inhibitors</i>	9
1.2.3.2 <i>The glial scar and inhibitory proteoglycans</i>	11
1.2.4 <i>Enhancing intrinsic growth pathways of CST neurons</i>	12
1.2.4.1 <i>MAPK/ERK pathway</i>	13
1.2.4.2 <i>Rho pathway inhibition</i>	14
1.2.4.3 <i>PI3K/Akt/mTOR pathway activation</i>	15
1.2.4.4 <i>Histone deacetylase inhibitors</i>	16
1.3 Histone Deacetylases and Their Inhibitors	16
1.3.1 <i>HDAC inhibitors</i>	18
1.3.2 <i>HDAC inhibitors can have neuroprotective effects</i>	19
1.3.3 <i>Relevance of HDACs and their inhibitors to CST neurons</i>	20
1.4 Rationale, Hypothesis and Aims	22
CHAPTER 2 : MATERIALS AND METHODS	25
2.1 Mice Used for Cell Culture: Thy-1YFP16JRS	25
2.2 Corticospinal Neuron Cell Culture	25
2.3 Immunocytochemistry	27
2.4 Image Analysis and Quantification	28
2.4.1 <i>Image acquisition</i>	28
2.4.2 <i>Neuron and corticospinal neuron counting using the cellomics automated microscope</i>	29
2.4.3 <i>Montaging and quantification of neurite length, branching and the number of primary neurites from individual neurons</i>	29
2.4.4 <i>Quantification of total CST neurite carpet outgrowth per field of view</i>	30
2.4.5 <i>Statistical analysis</i>	31
CHAPTER 3 : RESULTS	39
3.1 YFP Expression in P8 Thy1-YFP-16JRS Mice Demarcates a Population of Corticospinal Neurons in vivo, which is Maintained in vitro	39
3.2 Establishing Experimental Conditions with NT3, CNTF and HDAC Inhibitors	40

3.3	In the Presence of NT3 and CNTF, Tubastatin A and TSA Increase the Number of NST Positive and YFP Positive Neurons Respectively	41
3.4	Corticospinal Neuron Outgrowth, Branching and Primary Neurites in Response to Treatment with HDAC Inhibitors TSA and Tubastatin A	42
CHAPTER 4 : DISCUSSION		65
4.1	YFP Expressing Neurons Exhibit Characteristics of CST Neurons in vitro	65
4.2	YFP Expressing CST Neurons Respond to HDAC Inhibition in vitro	65
4.2.1	<i>HDAC inhibitor treatment increases the number of surviving corticospinal neurons in vitro</i>	65
4.2.2	<i>HDAC inhibitor treatment increased the number of primary neurites and branch points exhibited by corticospinal neurons in vitro</i>	67
4.2.3	<i>HDAC inhibitor treatment increased corticospinal neurite outgrowth in vitro.....</i>	68
4.3	Future Directions	71
4.3.1	<i>Establishing a purified population of CST neurons</i>	71
4.3.2	<i>Determining which specific HDACs are expressed by CST neurons in vitro.....</i>	72
4.3.3	<i>Determining whether the desired inhibitor of interest is causing transcription of previously silenced genes.....</i>	73
REFERENCES.....		74
APPENDICES		82
Appendix A.1 The Average Number of DAPI Positive Cells, Excluding Pyknotic Nuclei, Listed by Experiment		82
Appendix A.2 The Average Number of Excluded DAPI Positive Pyknotic Nuclei or Nuclear Fragments Listed by Experiment		83
Appendix A.3 The Average Number of NST Positive Neurons Listed by Experiment....		84
Appendix A.4 Average Number of GFP Positive Cells Listed by Experiment.....		85
Appendix A.5 Average Number of Primary Neurites per YFP Positive Neuron Listed by Experiment.....		86
Appendix A.6 Average Number of Branch Points per YFP Positive Neuron Listed by Experiment.....		87
Appendix A.7 Average Length (μm) of Neurite Outgrowth per YFP Positive Neuron Listed by Experiment		88
Appendix A.8 Average Length (μm) of YFP Positive Neurite Outgrowth per 20x Field of View Listed by Experiment		89

LIST OF TABLES

Table 2.1 Experimental Conditions for Addition of Growth Factors and HDAC Inhibitors.....	29
Table 2.2 Antibodies used for Immunocytochemical Assessment	30

LIST OF FIGURES

Figure 1.1 Histone Acetyltransferase and Histone Deacetylase Activity.....	24
Figure 2.1 YFP Expression in the Postnatal Day Eight Thy1 YFP-16JRS Mouse Identifies a Population Layer Five Projection Neurons.	34
Figure 2.2 The Optiprep™ Density Gradient Separates Cells Based on Density and Allows for the Isolation of a Neuronal Fraction.	35
Figure 2.3 DAPI Positive Pyknotic Nuclei and Cell Fragments Were Removed From Celloomics Analysis.....	36
Figure 2.4 Single Cell Outgrowth of Corticospinal Neurons can be Measured by ImageJ Skeletonization.....	37
Figure 2.5 Total Neurite Outgrowth of CST Neurons in a Field of View can be Measured by ImageJ Skeletonization.	38
Figure 3.1 YFP Positive Neurons Express Markers of Corticospinal Tract Neurons In Vitro.	45
Figure 3.2 The Culture System Contains Various Cell Types and a Consistent Population of NST Positive and YFP Positive Cells Across Experiments.	47
Figure 3.3 Preliminary Data Shows 10 nM TSA Treatment Increases YFP Positive Neurite Outgrowth.	49
Figure 3.4 Preliminary Data Shows 15 nM Tubastatin A Increases YFP+ Neurite Outgrowth (µm).	50
Figure 3.5 The Total Number of DAPI Positive Cells in Culture Increases in Response to TSA in the Absence of Growth Factors and When TSA or Tubastatin A Treatment is Delivered in the Presence of NT3+CNTF.	51
Figure 3.6 The Number of NST Positive Cells was Increased After Treatment With Tubastatin A in the Presence of NT3+CNTF.	53
Figure 3.7 The Number of Corticospinal Neurons Increased in Response to Treatment With TSA.....	55
Figure 3.8 Treatment With TSA Increased the Average Number of Primary Neurites of Corticospinal Tract Neurons.....	57
Figure 3.9 Corticospinal Neurite Branching is Increased in Response to TSA and Tubastatin A.....	59

Figure 3.10 Corticospinal Neuron Outgrowth per Cell was Increased in Response to Treatment With TSA or Tubastatin A. 61

Figure 3.11 Corticospinal Neuron Outgrowth per Field of View Increased in Response to Treatment With TSA or Tubastatin A in the Presence of NT3+CNTF. 63

LIST OF ABBREVIATIONS

DAPI	4',6-Diamidine-2-phenylindole dihydrochloride
DRG	Dorsal root ganglion
DIV	Days <i>in vitro</i>
BDNF	Brain-derived neurotrophic factor
CNS	Central nervous system
CNTF	Ciliary neurotrophic factor
CSPG	Chondroitin sulphate proteoglycan
CST	Corticospinal tract
CTIP2	Chicken ovalbumin upstream promoter transcription factor-interacting protein2
ERK/MAPK	Extracellular signal-regulated kinase/mitogen-activated protein kinase
FEZL	Forebrain embryonic zinc finger-like
ECM	Extracellular matrix
GAP43	Growth-associated protein 43
GFAP	Glial fibrillary acid protein
MAG	Myelin associated glycoprotein
MAP2	Micrtotubule associated protein 2
NGF	Nerve growth factor
NST	Neuron-specific tubulin, β III tubulin
NT3	Neurotrophin 3
OTX1	Orthodenticle homeobox 1
PI3K/Akt	Phosphatidylinositol 3-kinase/Akt

PLL	Poly-L-lysine
PNS	Peripheral nervous system
SCI	Spinal cord injury

ACKNOWLEDGEMENTS

First of all, I would like to thank my family and my fiancé Hamish; without your patience, love and support this would not have been possible.

To the members of the Roskams lab, thank you for being a surrogate family for me for the last three years; I truly appreciate your friendship. Thanks to our lab manager Nicole Janzen and my friend Kathryn Westendorf for always listening and offering sound advice on matters both personal and scientific. Thanks to Dr. Samantha Lloyd-Burton and Dr. Audrey Petit for being two of the most excellent sounding boards that a grad student could ever hope for. A special thanks to Sam for proof reading my thesis and setting me straight on the use of Em dashes—it's been a long time coming.

Thank you to Professor Roskams for allowing me the opportunity to work with such amazing people, this would not have been possible without your help and guidance.

I would also like to say a sincere thank you to my committee for being extremely helpful and facilitating the progression of my degree.

CHAPTER 1 : INTRODUCTION

1.1 Corticospinal Tract Neurons: Function, Development and Injury

The human corticospinal tract (CST) is responsible for coordinated voluntary movement and it contains descending afferent inputs involved in autonomic control, gating of spinal reflexes and nociception (Iwaniuk, Pellis, and Whishaw, 1999). After spinal cord injury (SCI), damage to the CST causes death and degeneration of axons and results in major motor impairments and sometimes even paralysis (Li and Raisman, 1995; Tom et al., 2004). The role of the rodent CST in gross motor function is not as well understood (Cheney, Fetz, and Mewes, 1991). Damage to the rodent CST leads to diminished contralateral forepaw coordination, forelimb weakness and minimal postural deficits (Lemon and Griffiths, 2005; Whishaw et al., 1993). Motor deficits present after SCI in humans are more severe compared to those observed in the rodent because rodents have additional descending tracts involved in motor control, which can compensate for injury to the CST (Whishaw et al., 1993).

The developmental profile of postnatal corticospinal neurons is similar in rodents and humans and the rodent is often used as a model system to investigate CST behaviour during development and injury (Fetz, 1968). Corticospinal neurons of a mouse are generated in the cortical neuroepithelium between embryological days 14-17 (E14-17) and most of them have migrated radially towards the cortical plate by E19-20 (Arlotta et al., 2005; Molnar and Cheung, 2006). During the early postnatal period the soma of these large pyramidal neurons are spread across layer five of the cortical mantle, becoming confined to rostral regions of

the cortex in adult animals (Joosten, 1997). These large pyramidal neurons produce a single apical dendrite, which terminates in cortical layer one and a few basal dendrites which project horizontally within layer five of the cortex (Terashima, 1995). Apical and basal corticospinal dendrites are spinous (Miller, Chiaia, and Rhoades, 1990). During early development corticospinal neurons express the transcription factors Ctip2 (COUP-TF interacting protein), Otx-1 (orthodenticle homeobox 1) and Fez1 (forebrain embryonic zinc finger-like), which are important for CST specification (Arlotta et al., 2005; Molyneaux et al., 2005). Once these neurons have reached their position in layer five of the sensory motor cortex they send out an axonal projection to the spinal cord via the striatum, internal capsule, cerebral peduncle and basilar pons (Molnar and Cheung, 2006). CST axons grow into the white matter synapse into grey matter in a staggered fashion so that leading CST fibres synapse in the upper cervical section at birth, midthoracic region by postnatal day 2 (P2) and the lumbar region at P5 (Fetz, 1968; Gianino et al., 1999). A small proportion of pioneer fibres are subsequently added to by a larger number of later arriving fibres (Joosten and Bar, 1999). Two days after arriving at their spinal target, CST fibres begin to branch into the gray matter and make connection with their targets (Gianino et al., 1999). CST fibers influence the activity of the motor neurons in the spinal cord directly, or indirectly through interneurons (Terashima, 1995). There are also minor portions of the CST (5-10% of fibres) that project ipsilaterally to the ventral cord and dorsal funiculi of the cervical cord (Gianino et al., 1999; Joosten and Bar, 1999; Terashima, 1995).

The intrinsic genetic program of CST neurons and the external environment surrounding their growing axons are both integral factors in the formation of appropriate connections with spinal targets. Ctip2 is a transcription factor important for early CST

specification and it is an important player for establishing appropriate CST outgrowth patterns; *Ctip2* null mice show defects in axon outgrowth and pathfinding (Arlotta et al., 2005). Target guidance is also accomplished by a host of external cues that can be either diffusible or contact mediated (Metin et al., 1997). Netrin 1 is an example of a diffusible chemoattractant that promotes axon growth in the vertebrate central nervous system (CNS), as it is responsible for the attraction of commissural axons towards the midline of the spinal cord (Kennedy et al., 1994; Metin et al., 1997). Semaphorin3A and netrin 1 are diffusible molecules which guide CST fibres through the midbrain towards the hindbrain during development (Finger et al., 2002) .

Glycoproteins present in extracellular matrix (ECM) and on cell surfaces have been shown to mediate the cell-cell interactions, which contribute to establishing correct CST outgrowth patterns (Joosten and Bar, 1999). N-cadherin, laminin, L1 and the neural cell adhesion molecule (NCAM) are all examples of adhesive molecules involved in the contact mediation of CST outgrowth (Joosten and Bar, 1999). NCAM and L1 have been extensively studied for their roles in CST outgrowth and will be discussed here. NCAM is an extracellular glycoprotein expressed on the axonal membrane of CST growth cones, which mediates cell-cell interactions and is important for the guidance of developing corticospinal axons (Hsu, Stein, and Xu, 2005). CST pathfinding errors occur in NCAM deficient mice (Cohen et al., 1998). L1 is another glycoprotein which is important for the growing CST, and it has been found to mediate neuron-neuron interactions in the CST fibres which arrive after the pioneer axons (Joosten and Bar 1999; Cohen et al., 1998). The CST fibres of L1 deficient mice show pathfinding errors—there is a reduced number of CST

axons in the dorsal columns and these neurites do not extend past the cervical cord (Cohen et al., 1998).

In addition to guidance cues for appropriate pathfinding, CST neurons also require growth factors, which can promote outgrowth and survival, in order to reach their final destination. Neurotrophin-3 (NT3) can be involved in coordinating CST innervation of the midbrain during development (Joosten and Bar 1999). Insulin like growth factor 1 (IGF1) has also been shown to be critical for axon outgrowth during initial CST development (Ozdinler and Macklis, 2006). Neurotrophins such as ciliary neurotrophic factor (CNTF), glial derived neurotrophic factor (GDNF), NT3 and neurotrophin 4 (NT4) support the survival of corticospinal neurons grown in mixed cortical cultures *in vitro* (Giehl, 2001; Junger and Junger 1998).

In general, the CST responds to injury by degeneration and axon retraction (Li and Raisman, 1995; Tom et al., 2004). Injured corticospinal axons also exhibit impaired axonal transport and pathological axolemma permeability (Hill, Beattie, and Bresnahan, 2001). This cascade of degeneration results in the failure of CST axons to regenerate, leaving them unable to re-form meaningful connections with their targets (Li and Raisman, 1995; Tom et al., 2004). Unlike neurons of the peripheral nervous system (PNS), CST neurons fail to increase the expression of growth associated genes such as the axonal growth associated protein 43 (GAP 43) (Tetzlaff et al., 1991) and CAP 43 (Tedeschi et al., 2009) after injury. The expression of growth associated genes may indeed be a requirement for successful axonal regeneration post injury (Tetzlaff et al., 1991).

1.2 Spinal Cord Injury: Barriers to Regeneration and Therapeutic Strategies

SCI often results in severe impairment of sensory, loco-motor and autonomic functions; the most brutal injuries can leave the patient paralyzed and incontinent for a lifetime (Looby and Flanders, 2011). SCI is most common in young- middle age adults (Looby and Flanders, 2011) and unfortunately, the adult mammalian CNS is lacking in its ability to regenerate after injury (Anderson and Lieberman, 1999; Chong et al., 1996). Injuries to the adult CNS result in degeneration of transected axons, which form dystrophic end bulbs and ultimately fail to regrow through the site of injury (Li and Raisman, 1995; Tom et al., 2004). The motor deficits observed after SCI are in part due to injury incurred by CST (Fetz, 1968), which is particularly deficient in its ability to regenerate post injury (Fishman and Kelley, 1984; Liu et al., 2010). The lack of regeneration in the CNS after trauma is due to a combination of factors: the lesion cavity, the absence of neurotrophic growth-supporting molecules (Berry, Carlile, and Hunter, 1996; Bradbury et al., 1999), the hostile growth environment in the lesion site (Hunt, Coffin, and Anderson, 2002) and the inadequate intrinsic capacity for outgrowth of adult CNS neurons (Anderson and Lieberman, 1999; Chong et al., 1996).

1.2.1 Bridging the lesion gap with cell therapies

There is a physical gap in the tissue left behind after trauma, which is exacerbated by the death and degeneration of transected axons in the lesion core (Ramer, Ramer, and Steeves, 2005). The injury cavity is physically hard to traverse for neurons, which ultimately

require complex networks of ECM and cell-cell contact in order to extend neurites. Glial cell transplants have been used as a potential SCI therapy because the transplanted cells are able to fill the lesion space providing a bridge over which the process extension can occur as well as remyelinating demyelinated tracts and potentially secreting neurotrophic factors to support neurite outgrowth (Ramer, Ramer, and Steeves, 2005; Tetzlaff et al., 2010). Glia from the PNS (Schwann cells [SC]) and the CNS (olfactory ensheathing cells [OECs]) have been transplanted into the lesion site and have produced variable amounts of axon regeneration (Richter and Roskams, 2008; Tetzlaff et al., 2010). While SC grafts have been able to promote outgrowth of sensory axons and propriospinal axons close to the injury site, there has been no evidence of long distance axon regeneration through SC bridges (Tetzlaff et al., 2010). Corticospinal tract fibres are particularly unresponsive to SC transplantation (Guest et al., 1997; Tetzlaff et al., 2010).

OECs are better able to integrate into the host tissue compared to SCs and have been shown to increase long distance axonal sprouting of CST neurons (Ramon-Cueto et al., 2000). However, other studies have not been able to reproduce this effect and have shown no regeneration of fibers below the site of injury (Kubasak et al., 2008). Some studies have even demonstrated that OECs transplanted into sites of spinal cord lesion stimulate sprouting of tyrosine hydroxylase positive fibers, which could be responsible for nociception (Ramer et al., 2004). The variability in the existing body of literature regarding behavioural outcomes and reports of axonal regeneration could be attributable to disparate tissue sources (olfactory bulb derived OECs or lamina propria derived OECs from different ages) or it might be due to the way that OECs are cultured (Richter and Roskams, 2008; Tetzlaff et al., 2010). Quite often glial cell transplants have to be combined with some other

cell type or some neurotrophic factor to make a significant difference in outgrowth (Tetzlaff et al., 2010).

Neural stem cells and progenitors (NPSCs) have also been transplanted into sites of spinal cord lesion in the hopes that they will confer the lesion site with the permissive growth environment of the embryo (Ramer, Ramer, and Steeves, 2005; Tetzlaff et al., 2010). There is also some speculation that the transplanted cells might be able to receive synaptic input from regenerating axons and relay information to the other side of the lesion (Ramer, Ramer, and Steeves, 2005). Once transplanted, these cells mostly differentiated into oligodendrocytes and astrocytes, with a small percentage of them giving rise to new neurons (Parr et al., 2008). While there has been some functional recovery reported in various lesion models, NPSCs have not been able to support axonal regeneration through the lesion site (Tetzlaff et al., 2010). Much like OECs and SCs, there is variability in how NPSCs are harvested, cultured and transplanted into the lesion site. Commonly NPSC transplantation occurs in concert with co-application of other treatments such as neurotrophic factors (Sato and Oohira, 2009).

Most cell transplantation studies have been performed in the rodent and have used acute injury models (Tetzlaff et al., 2010). Unfortunately there is often very little functional recovery reported in studies employing chronic treatments; this is problematic as cell transplant therapies are touted as treatment options for patients with chronic SCI (Tetzlaff et al., 2010).

1.2.2 Neurotrophic support

Most of the original work investigating neurotrophin signaling used PC12 cells as a model system and showed that nerve growth factor (NGF) promotes survival and induces PC12 differentiation, causing these cells to extend neurites (Tischler and Greene, 1975). Neurotrophic factors commonly bind to neuronal tyrosine kinase receptors (trkR) and through various intracellular signaling events come to affect neuronal survival and neurite outgrowth (Lu, Blesch, and Tuszynski, 2001). More recent work has employed the use of primary sensory and sympathetic neurons *in vitro* to investigate the intracellular signaling cascades activated by neurotrophins. The signaling cascades transducing-neurotrophin mediated survival or outgrowth are not always similar between different cell types. While the neurite outgrowth observed after NGF application was largely due to activation of the extracellular signal-regulated kinase/mitogen-activated protein kinase (ERK/MAPK) in PC12 cells the same was not true for primary sensory neurons (Kleese 1999). Activation of the phosphatidylinositol 3-kinase/Akt (PI3K/Akt) cascade or the Ras G-protein was sufficient for promoting sensory neuron survival but the downstream members of the ERK cascade were not involved (Klesse, 1999). The above example stresses the importance of investigating the effects of neurotrophins in the target neurons of interest. In the CST, neurotrophins such as CNTF, NT-4 and GDNF, but not NGF, NT3 or brain derived neurotrophic factor (BDNF) have been shown to support neuron survival in an enriched culture of neonatal rat cortical neurons (Junger and Junger, 1998). In a more pure population of fluorescence activated cell sorting (FACS) purified rat neonatal corticospinal neurons, both CNTF and GDNF can promote neuron survival (Junger and Junger, 1998). Furthermore, NT3 and BDNF, but not NGF have survival promoting effects when delivered

via osmotic pump to corticospinal neurons axotomized at the level of the internal capsule *in vivo* (Giehl and Tetzlaff, 1996). Although BDNF can promote survival and collateral sprouting but is not able to promote long range outgrowth of CST neurons post injury (Lu, Blesch, and Tuszynski, 2001; Hiebert et al., 2002). After SCI, NGF can promote axon growth in coeruleospinal and sensory neurons but not in CST neurons (Weidner et al., 1999). NT3 can be neuroprotective and promote short-range sprouting of transected CST fibres (Ozdinler and Macklis, 2006; Schnell et al., 1994). However, treatment with either a single NT3 application or transplantation of hyper-NT3-secreting fibroblast grafts after SCI failed to promote CST fibre extension through the host white matter (Grill et al., 1997). Taken together, neurotrophins are able to promote local sprouting after injury but are not sufficient to promote long-range regeneration of CST fibres after SCI (McKerracher and Higuchi, 2006). The therapeutic potential for neurotrophins may be reliant on their ability to promote sprouting, reinnervation and remodeling of local circuits rather than long distance growth (McKerracher and Higuchi, 2006).

1.2.3 Neutralizing the inhibitory lesion environment

1.2.3.1 Myelin associated inhibitors

Trauma damages the myelin sheath surrounding axons and results in myelin fragmentation immediately after injury (Fawcett and Asher, 1999). The myelin debris released into the surrounding area can be inhibitory to neurite outgrowth (Fawcett and Asher, 1999; Hunt, Coffin, and Anderson, 2002). Myelin *in vivo* and mature oligodendrocytes *in vitro* contain three molecules which have been implicated in the inhibition of axon growth: Myelin-associated glycoprotein (MAG), Oligodendrocyte-myelin

glycoprotein (OMpg) and Nogo (Caroni, Savio, and Schwab, 1988; Fawcett and Asher, 1999; Hunt, Coffin, and Anderson, 2002; Richter and Roskams, 2009). Oligodendrocytes begin to express MAG and OMpg at the onset of axon myelination (Hunt, Coffin, and Anderson, 2002; Nash et al., 2009). MAG is thought to be important for the development and maintenance of myelinated axons while OMpg is involved in membrane adhesion at the nodes of Ranvier (Nash et al., 2009). The myelin of both MAG and OMpg knockout mice is more growth permitting than the myelin of control mice, however, there has been no report of CST regeneration in these knockout mice (Nash et al., 2009). On the other hand, most experiments which use function blocking antibodies aimed at neutralizing the inhibitory effects of Nogo-A involve the CST (Hunt, Coffin, and Anderson, 2002; Schnell and Schwab, 1990). Nogo exists in three main isoforms in the adult CNS and is a cell surface protein expressed by oligodendrocytes and some neuronal subtypes (Hunt, Coffin, and Anderson, 2002). Inhibition of Nogo using a function blocking antibody results in the outgrowth of transected CST neurons in postnatal rats after dorsal hemisection (Schnell and Schwab, 1990). However, this partial lesion model does not preclude the fact that the outgrowth may be attributable to sprouting from spared fibres instead of regeneration of transected axons (Hunt, Coffin, and Anderson, 2002). The increased CST outgrowth seen by Schnell et al. (1990) has yet to be reproduced in a model more similar to human SCI such as a complete transection, a contusion or a compression injury (Hunt, Coffin, and Anderson, 2002). Furthermore, the fact that neurons themselves, including CST neurons, express Nogo makes one wonder what effects Nogo inhibition is having on the normal function of intact neurons affected by the antibody (Nash et al., 2009).

1.2.3.2 The glial scar and inhibitory proteoglycans

One of the major barriers to regeneration occurs in the form of a glial scar which surrounds the lesion site (Fitch and Silver, 2008; Silver and Miller, 2004). In response to trauma, astrocytes begin to divide, become hypertrophic and migrate towards the lesion site, in an attempt to surround and protect the fragile CNS tissue (Fawcett and Asher, 1999; Silver and Miller, 2004). The glial scar is mostly made up of reactive astrocytes and basal lamina but it also contains some oligodendrocytes and microglia (Iseda et al., 2003). Over time the scar tissue becomes an increasingly tough-growth-blocking membrane, which is inhibitory to axon growth due to its physical properties (Windle and Chambers, 1950) and due to the inhibitory molecules it contains within its matrix (Fawcett and Asher, 1999; Fitch and Silver, 2008). After injury, reactive astrocytes up-regulate a host of different molecules, such as chondroitin sulfate proteoglycans (CSPGs), which are inhibitory to axon regeneration (Fitch and Silver, 1997; Haas et al., 1999). Enzymes geared toward inactivating CSPGs have been used in the hopes that they will render the inhibitory lesion environment more conducive to promoting neurite outgrowth. Chondroitinase enzymes remove most of the sugar chains from CSPGs leaving the protein core and carbohydrate stub; this decreases the inhibitory properties of CSPGs (Silver and Miller, 2004). The digestion of CSPGs by chondroitinase enzymes can promote sensory and motor axon regrowth through the lesion site when applied to animals with bilateral dorsal column lesions (Silver and Miller, 2004). This treatment also resulted in the recovery of some sensory and loco-motor functions (Silver and Miller, 2004). While there have been positive results using the hemisection lesion model there has been no increase in axon outgrowth observed in the contusion model of SCI (Iseda et al., 2008). In fact, in the contused spinal

cord, CST axons retract and are unable to grow through the CSPG neutralized glial scar (Iseda et al., 2008).

1.2.4 Enhancing intrinsic growth pathways of CST neurons

After insult, the long myelinated tracts of the CNS are only capable of stunted axon sprouting and they tend to form dystrophic end bulbs which behave like stalled growth cones (Guth et al., 1985; Li and Raisman, 1995). This short-range sprouting is not sufficient to reinstate functional circuitry (Fitch and Silver, 2008). The long myelinated tracts of the CST have proven to be particularly deficient of the capacity for meaningful regeneration post injury (Fishman and Kelley, 1984). Attempts have been made to regenerate CST fibres by making the inhibitory lesion environment more amenable to axon growth (Cadotte and Fehlings, 2011; Caroni, Savio, and Schwab, 1988). However, neutralizing the inhibitory lesion environment or providing increased trophic support to injured CST neurons may improve short range sprouting but it is not sufficient to support meaningful long-range outgrowth. This suggests that it is most important to focus on understanding the intrinsic capacity for neurons to regenerate—irrespective of their surroundings. Neurite outgrowth can be modulated at the level of neuronal transcription or by alterations in the various intracellular signaling cascades active within the cell. A number of intrinsic signaling pathways are important for neurite outgrowth during development, including: P13K/Akt/mTOR (Goldberg et al., 2002), MAPK/ERK (Huang and Reichardt, 2003) and the Rho/Rho-associated protein kinase (ROCK) cascades (Fournier, Takizawa, and Strittmatter, 2003). Histone deacetylase enzymes (HDACs) are involved in transcription regulation and gene silencing (Morrison, Majdzadeh, and D'Mello, 2007) and inhibition of

these enzymes can promote neurite outgrowth. The role of these intrinsic neurite outgrowth promoters in relation to corticospinal fibre regeneration will be discussed below.

1.2.4.1 MAPK/ERK pathway

As mentioned previously, neurotrophins have been shown to activate the MAPK/ERK pathway in PC12 cells (Kleese 1999). The MAPK/ERK pathway has been implicated in neurite outgrowth in the PNS and retinal ganglion cells (RGCs) (Goldberg et al., 2002). A previous study investigating the effects of IGF-1 on neurite outgrowth of FACS purified rat corticospinal neurons implicated the MAPK/ERK pathway in IGF-1-mediated promotion of neurite outgrowth (Ozdinler and Macklis, 2006). The level of phospho-ERK increased in response to IGF treatment compared to un-treated controls and the inhibition of ERK (PD 98059 inhibitor) significantly reduced the amount of axon growth present after IGF-1 treatment (Ozdinler and Macklis, 2006). This directly implicates ERK signaling in corticospinal outgrowth pathways. Other research has demonstrated that ERK is involved in corticospinal neurite extension *in vivo* (Hollis et al., 2009). Lentiviral overexpression of the BDNF receptor trkB in layer 5 of the motor cortex resulted in greater corticospinal fibre extension in response to BDNF after injury (Hollis et al., 2009). This increase in outgrowth was diminished in response to inhibition of the ERK pathway (Hollis et al., 2009).

1.2.4.2 *Rho pathway inhibition*

Rho is a small GTPase that is part of the Ras superfamily of proteins. The Rho subfamily consists of RhoA, Cdc42 and Rac, all of which have effects on actin cytoskeletal dynamics (Kouchi et al., 2011). Cdc42 and Rac activity promotes neurite outgrowth, whereas, the activation of Rho inhibits neurite outgrowth and actually promotes neurite retraction (Kouchi et al., 2011). A careful interplay between the Rho family of GTPases is necessary for the appropriate growth and wiring of the nervous system during development and regeneration.

Neurotrophins have been shown to increase intracellular cyclic adenosine monophosphate (cAMP), which phosphorylates protein kinase A (PKA), resulting in the inactivation of Rho in RGCs (Monsul et al., 2004). Increases in intracellular cAMP or neutralization of Rho may allow neurons to grow in the inhibitory lesion environment. After injury, inhibitory molecules in the glial scar confer their inhibitory effects through the Rho-Rock pathway (Fournier, Takizawa, and Strittmatter, 2003; Lingor et al., 2007). Myelin fragments and CSPGs activate Rho and its downstream effector ROCK, which in turn phosphorylates the myosin light chain (MLC) leading to actin contractility, growth cone collapse and neurite retraction (Hunt, Coffin, and Anderson, 2002; Lingor et al., 2007). Inhibitors of the Rho-Rock pathway have been shown to increase neurite outgrowth in the injured CNS (Fournier, Takizawa, and Strittmatter, 2003). More specifically, Rock inhibitors (Y-27632) increase neurite extension in the presence of CSPGs *in vitro* and in RGCs *in vivo* (Lingor et al., 2007; Borrisoff et al., 2003). Neutralizing Rho and Rock using the inhibitors C3 and Y-27632 respectively increases outgrowth of embryonic cortical neurons grown in the presence of CSPGs and myelin *in vitro* (Dergham et al., 2002). The

immediate application of C3 or Y-27632 to the partially transected spinal cord increased CST fibre growth and functional recovery post injury (Dergham et al., 2002).

1.2.4.3 PI3K/Akt/mTOR pathway activation

Neurotrophins such as NGF have been shown to activate the PI3K/Akt/mTOR pathway in primary sensory neurons and RGCs (Kleese 1999). IGF-1 can have outgrowth promoting effects on FACS purified corticospinal neurons, this increase in neurite outgrowth is reduced after application of the PI3K inhibitor (LY 294002) (Ozdinler and Macklis, 2006).

The phosphatase and tensin homologue (PTEN) is a negative regulator of the mTOR pathway which is involved in controlling cell growth (Park et al., 2008). mTOR is downregulated with age and injury and this decrease correlates with the diminished regenerative capacity of aged cortical neurons (Park et al., 2008). Conditional deletion of PTEN in postnatal mice (P1) increases mTOR expression and promotes axon regeneration in retinal ganglion cells (RGCs) of adult mice (Park et al., 2008). Using the same model of PTEN deletion the group also reported a robust increase in CST fibre regeneration in both incomplete (dorsal hemisection) and complete crush models of SCI (Liu et al., 2010). This CST fibre regeneration was seen in both young and old animals (5 months) after both acute and chronic treatment paradigms (Liu et al., 2010). The increased regeneration in PTEN-deleted CST neurons was concurrent with an increase in excitatory synapse formation (Liu et al., 2010). This study is perhaps one of the most thorough and promising in a field trying to promote CST regeneration, however, they have yet to show that the synapses formed are functionally operational and lead to behavioural recovery.

1.2.4.4 Histone deacetylase inhibitors

HDACs remove the acetyl groups from histones resulting in DNA compaction and transcriptional repression (Morrison, Majdzadeh, and D'Mello, 2007).

Inhibitors aimed at neutralizing the effects of HDACs have been used to try to promote outgrowth of mature CNS neurons in the hopes that they can reverse the developmental shift towards a non-regenerative phenotype by allowing the re-expression of genes involved in the neurite outgrowth program that are no longer expressed in the mature CNS. Valproic acid (VPA) is an HDAC inhibitor which can have neuroprotective effects on lower motor neurons (Ragancokova et al., 2009). Other HDAC inhibitors like TSA and Tubascin have been shown to have both neuroprotective and neurite outgrowth promoting effects on embryonic cortical neurons *in vitro* in the presence of inhibitory molecules like MAG (Rivieccio et al., 2009). To date, there have been no studies which have directly investigated the effects of HDAC inhibitors on outgrowth of CST neurons specifically.

The above section was intended to give a brief introduction to HDACs and to provide examples of studies which promote neurite outgrowth. For a more in depth review of HDACs, their inhibitors and their mechanisms of action see section 1.3.

1.3 Histone Deacytelases and Their Inhibitors

Gene transcription is partly mediated by an antagonistic interplay between histone acetyl transferase (HAT) and HDAC activity (Kazantsev and Thompson, 2008; Wang and Zhang, 2009) (Figure 1.1). HATs add acetyl groups to the lysine residues of the histones contained within the nucleosome, causing chromatin to adopt an open configuration and promoting transcription (Morrison et al., 2006). In contrast, HDACs remove acetyl groups

from histones, causing chromatin compaction and diminished accessibility of transcription factors; this leads to gene silencing (Kazantsev and Thompson, 2008). HDACs also deacetylate non-histone proteins such as p53 and α -tubulin and have been implicated in multiple cellular processes such as differentiation, cell survival and cell death (Morrison, Majdzadeh, and D'Mello, 2007; Suzuki, 2009). HDACs are grouped into three classes based on their homology to yeast orthologs (Wang and Zhang, 2009). There is a remarkable degree of structural similarity between class I and II HDACs, which both exhibit zinc dependent catalytic activity (Kazantsev and Thompson, 2008). Class I HDACs are mainly found in the nucleus and include HDAC 1,2,3 and the muscle specific HDAC 8 (Kazantsev and Thompson, 2008). HDACs 1 and 2 are perhaps the best characterized class I isoforms and they exist in the transcriptional complexes such as NuRD (Zhang et al., 1999). These complexes are recruited to gene promoters by DNA binding proteins, which suggests gene specific rather than global transcriptional regulation (Kazantsev and Thompson, 2008). Few researchers have explored the expression patterns of HDACs in specific cell types. However, MacDonald *et al.* (2008) revealed that HDAC1 is expressed in radial glia, and progenitors in the brain and spinal cord. HDAC 2 is expressed in post-mitotic immature neurons and is down-regulated as they become mature (MacDonald and Roskams, 2008).

Class II HDACs (HDAC 4,5,6,7 and 11) shuttle between the cytoplasm and nucleus in response to cellular signals (Dokmanovic and Marks, 2005; Morrison et al., 2006). HDACs from class I are more ubiquitously expressed compared to class II HDACs (Kazantsev and Thompson, 2008). Since class I HDACs are broadly expressed in the CNS and other tissues it suggests a wide role for these enzymes in controlling transcription and argues against a neuron specific function. Conversely, class II HDACs are highly expressed in the brain and

can be further broken down into subclasses IIa (4,5 and 7) and IIb (6 and 10) (Kazantsev and Thompson, 2008). Interestingly, HDAC 6 is the only isoform that contains two catalytic domains and functions primarily in the cytoplasm where it can sometimes deacetylate alpha tubulin and alter microtubule stability (Southwood et al., 2007; Zhang et al., 2003). HDAC 6 is expressed in many post-mitotic neurons and is especially abundant in Purkinje cells (Southwood et al., 2007)

The sirtuins (SIRT) make up class III HDACs, and their catalytic activity is dependent on a nicotinamide adenine dinucleotide (NAD⁺) mechanism (Kazantsev and Thompson, 2008). The SIRTs do not usually deacetylate histones in mammalian cells and so are not considered to be classical HDACs and will not be discussed further in this section (Morrison, Majdzadeh, and D'Mello, 2007).

1.3.1 HDAC inhibitors

A multitude of synthetic small molecules and naturally occurring compounds have been identified as HDAC inhibitors. Initially, most HDAC inhibitors were explored for their potential as anticancer therapeutics (Kazantsev and Thompson, 2008) but have since been expanded to include CNS pathologies such as Huntington's disease (HD) and amyotrophic lateral sclerosis (ALS) (Petri et al., 2006; Steffan et al., 2001). Inhibitors of the class I and II HDACs are organized into different groups based on their chemical structure; these include short chain fatty acids (carboxylic acids), hydroxamates and benzamides (MacDonald and Roskams, 2009). Many of the commonly used HDAC inhibitors are pan-HDAC inhibitors, which neutralize the activity of many, if not all, of the HDAC isoforms in class I and II (Morrison, Majdzadeh, and D'Mello, 2007). Valproic Acid (VPA) is a short

chain fatty acid and is perhaps the most widely used pan-HDAC inhibitor *in vivo* (MacDonald and Roskams, 2009). VPA was originally used as an antiepileptic drug and is now in clinical cancer trials (Dokmanovic and Marks, 2005; Ragancokova et al., 2009). Inhibition with VPA is not specific to HDACs, as VPA also exerts effects on GABAergic transmission and inflammation (Johannessen, 2000). Hydroxamate inhibitors such as suberoylanilide hydroxamic acid (SAHA) and TSA, have fewer off target effects and effectively inhibit all the class I and II HDAC isoforms (Dokmanovic and Marks, 2005). Hydroxamate inhibitors exert their effects by chelating the zinc ion in the active site of HDACs, thereby rendering them inactive (Kazantsev and Thompson, 2008). Isoform selective inhibitors are becoming increasingly common and are designed on the basis of the three-dimensional shape of the HDAC active site instead of relying on zinc chelation (Kazantsev and Thompson, 2008; Suzuki, 2009). A benzamide derivative called MS-275 inhibits HDAC 1 preferentially over HDACs 2,3 and 9 and has little effect on HDACs 4,6,7 and 8 (Chuang et al., 2009). Tubastatin A and Tubascin are both isoform specific inhibitors of HDAC 6, an isoform which is located in the cytoplasm and can deacetylate alpha tubulin, cortactin and heat shock protein 90 (HSP90) (Rivieccio et al., 2009; Suzuki, 2009; Zhang et al., 2003).

1.3.2 HDAC inhibitors can have neuroprotective effects

HDAC inhibitors have been shown to exert neuroprotective effects *in vivo* and *in vitro* (Chuang et al., 2009). Treatment with HDAC inhibitors can ameliorate the symptoms associated with various neuropsychiatric and neurodegenerative disorders such as depression, HD and ALS (Petri et al., 2006; Steffan et al., 2001). However, the

neuroprotective actions of HDAC inhibitors in disease have been poorly characterized (Uo, Veenstra, and Morrison, 2009).

The neuroprotective effects of HDAC inhibitors have been more thoroughly characterized *in vitro*. Cortical neuron cultures treated with TSA, SAHA or sodium butyrate showed increased survival in a glutathione depletion model of oxidative stress (Ryu et al., 2003). Application of TSA or Tubastatin A has also been shown to promote cortical neuron survival in the face of oxidative stress by Ratan and colleagues (2009). While some studies have reported certain levels of toxicity after prolonged TSA treatment, this can be avoided by using a short term pulse treatment paradigm (Langley et al., 2008). Multiple mechanisms have been put forward to account for the neuroprotective effects conferred by HDAC inhibitor treatment. Multiple groups have demonstrated that VPA can induce BDNF expression in both neurons and astrocytes *in vitro* (Wu et al., 2008; Yasuda et al., 2009) and BDNF has previously been shown to promote survival of various types of neurons *in vitro* and *in vivo*. Treatment with either VPA or MS-275 activated the promoter of HSP70 in cortical neurons; HSP70 is an important cytoprotective protein that has anti-apoptotic and anti-inflammatory effects (Marinova et al., 2011). Another study illustrated that inhibition of class I and II HDACs using TSA and SAHA blocked Bax-dependent apoptosis in postnatal mouse cortical neurons (Uo, Veenstra, and Morrison, 2009).

1.3.3 Relevance of HDACs and their inhibitors to CST neurons

Inhibitors aimed at neutralizing the effects of HDACs can promote the expression of previously silenced genes. Therefore, HDACs may be able to reinstate the expression profile necessary to promote regeneration in CST neurons that have been shown to be refractory to regeneration after injury. Little is known about the expression patterns of the

traditional HDACs in the major projection neurons of the motor system. However Topark-
Ngarm *et al.* (2006) showed that Ctip2—previously identified as an integral transcription
factor for CST specification—associates with the NuRD repressor complex which contains
HDACs 1 and 2. HDAC activity in Ctip2 positive neurons is inhibited by TSA *in vitro*
(Topark-Ngarm *et al.*, 2006). Histone deacetylase and chromatin remodeling activities of
NuRD may be implicated in the regulation of CST specification, development, and
outgrowth mediated by Ctip2.

As mentioned above, TSA can have neurite outgrowth promoting effects on mixed rat
embryonic cortical neurons *in vitro* (Rivieccio *et al.*, 2009). Although the study was not
specifically assessing the outgrowth response of CST neurons, a subcomponent of the
culture may have contained CST neurons. Interestingly, in this study there was no increase
in neurite outgrowth after application of a class one specific inhibitor—sodium butyrate.
This led investigators to conclude that the outgrowth response was attributable to inhibition
of class 2 HDACs. Quantitative polymerase chain reaction (PCR) studies showed an
increase in HDAC 6 expression in response to oxidative stress and neurite outgrowth
inhibitors, suggesting that HDAC 6 might be a key player in modulating the neuronal
response to pathology (Rivieccio *et al.*, 2009). Indeed, the pharmacological inhibition and
small interfering RNA (siRNA) knockdown of HDAC 6 rendered the enzyme inactive and
resulted in increased neurite outgrowth (Rivieccio *et al.*, 2009).

1.4 Rationale, Hypothesis and Aims

The adult CNS is severely deficient in its ability to regenerate after injury and this has been postulated to be partly attributable to the silencing of genes that are important for neuronal outgrowth during development. It has been shown previously in our lab that as olfactory neurons mature, GAP43, an important growth associated protein during development and regeneration, is silenced by methylation and HDAC 1 and 2 activity (Macdonald et al., 2010). This study directly implicates HDAC activity in the repression of neurite growth associated genes in mature neurons. Another study showed that application of the HDAC inhibitor TSA resulted in hyperacetylation of histone 3, neurite outgrowth and an increase in the expression of GAP43 in postnatal cerebral granular neurons (Gaub et al., 2010) This increase in GAP43 expression was abolished when TSA was applied in concert with the transcriptional repressor flavopiridol, suggesting that the observed hyperacetylation-mediated increase in GAP43 expression and neurite growth were dependent on transcription (Gaub et al., 2010). In addition to TSA, the HDAC 6 isoform specific inhibitor Tubastatin A, has also both been shown to promote outgrowth of rat embryonic cortical neurons *in vitro* (Rivieccio et al., 2009).

As mentioned previously, HDAC activity has been linked to corticospinal neurons in a study that showed that neurons expressing Ctip2, a transcription factor integral for CST development, express HDAC 1 and 2 and are indeed sensitive to HDAC inhibition by TSA (Topark-Ngarm et al., 2006). HDAC inhibitors have been shown to exert neuroprotective effects *in vivo* and *in vitro* (Chuang et al., 2009). Treatment with TSA, SAHA or Tubastatin A can increase survival of cortical neurons in a model of oxidative stress (Rivieccio et al., 2009; Ryu et al., 2003). Taken together, HDAC inhibitors have the ability to: i) promote

neuronal survival in cortical neurons; ii) promote neurite outgrowth and an increase in outgrowth associated protein expression in non-CST neurons; and iii) are able alter CtIP2 activity-an important player in CST specification during development.

It is important to investigate the regenerative capacity of more mature neurons in response to axotomy as it is the mature CNS that is deficient of the intrinsic capacity for regeneration after injury. Therefore, we chose to investigate whether more mature P8 CST neurons, which have already made synaptic contact with their targets in the spinal cord, could display an increase in survival and neurite outgrowth in response to treatment with the HDAC inhibitors TSA and Tubastatin A.

HYPOTHESIS: CST neurons will display increased survival and neurite outgrowth in response to application of HDAC inhibitors.

AIM 1: To establish and characterize a CST neuron culture system.

AIM 2: To determine if HDAC inhibitors can promote survival and neurite outgrowth in CST neurons in this culture system.

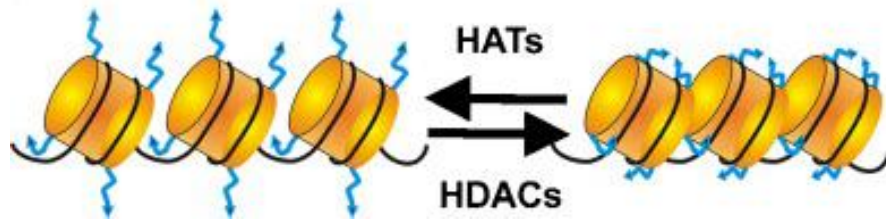


Figure 1.1 Histone Acetyltransferase and Histone Deacetylase Activity

(Adapted from MacDonald and Roskams, 2009) Histone acetylases (HATs) add acetyl groups to the lysine residues of the core histones contained within a nucleosome causing chromatin to adopt a more relaxed configuration and permitting transcription. Histone deacetylases (HDACs) remove acetyl groups from histones leading to chromatin compaction and gene silencing.

CHAPTER 2 : MATERIALS AND METHODS

2.1 Mice Used for Cell Culture: Thy-1YFP16JRS

All studies were performed under the approval and guidelines of the Canadian Council for Animal Care, and the Animal Care Committee of the University of British Columbia.

Thy1-YFP16JRS mice were purchased from the Jackson Laboratory as heterozygotes. These mice were generated using the murine Thy1 vector, containing the murine Thy1.2 gene from its promoter to the intron following exon 4, but exon 3 and its flanking introns were removed. Exon three is required for non-neuronal expression, therefore this vector, driving YFP results in YFP expression in neuronal cells (Feng, et al., 2000). Previously in the lab heterozygotes were genotyped and crossed with other heterozygotes to generate homozygote mice. Homozygosity was confirmed by breeding potential homozygote mice with WT CD-1 mice, and examining two of the resulting litters (13 pup minimum) to confirm cortical expression of YFP by epifluorescence. Previous work in the lab demonstrated that Thy1-YFP16JRS mice have vibrant YFP in layer 5 cortical neurons and that these neurons express CST transcription factors Ctip2 and Otx1 (Figure 2.1)(Richter and Roskams, 2009).

2.2 Corticospinal Neuron Cell Culture

For each experiment, four or five P8 Thy1-YFP16JRS mice were decapitated one at a time, and their brains were dissected from the skull and placed in ice cold HibernateTM containing 1X B27TM and 0.5mM L-glutamine (HABG, all from Invitrogen). Each brain

was microdissected by stereotaxically slicing the brain along the coronal axis at 1mm and then 2mm caudal from the most rostral surface of the cortex so that two 1mm thick coronal sections were collected. Microforceps were used to remove the meninges from the surface of the brain and to cut away the corpus callosum and brainstem structures from the cortex. The cortex was then cut 2-2.5mm lateral from the midline on each side of the brain. The pieces of cortex were collected and cut into smaller pieces measuring approximately 0.5mm each along the axis of the cortical surface. The pieces of cortex were digested in papain (30U per ml, Worthington PAP2), in complete HBSS containing 1X HBSS (Invitrogen), 1% PenStrep (P/S; Invitrogen), 2.5 mM HEPES (Invitrogen), 30 mM D-Glucose (Sigma), 1 mM CaCl₂, 1 mM MgSO₄, 4 mM NaHCO₃ (all from Fischer) for 30 minutes at 30°C with gentle oscillation. The digestion solution was removed and replaced with 5ml of 30°C HABG and kept for five minutes at room temperature. A fire polished Pasteur pipette was used to mechanically dissociate the tissue by triturating 10 times, allowing the pieces to settle for one minute before collecting the supernatant. The trituration steps were repeated three times in order to collect the maximum number of cells while being as gentle as possible with the cell solution. The cell suspension was layered on top of a four layer Optiprep™ (Sigma)-HABG gradient (bottom layer 1 = 1.1014 g/ml, layer 2 = 1.0397 g/ml, layer 3 = 1.0317g/ml, top layer 4 = 1.0237 g/ml) and centrifuged at 1,900 r.p.m for 15minutes at 22°C. Cellular debris and the oligodendrocyte fraction were removed and discarded using a P1000 pipette (Figure 2.2). The second and third fractions were enriched for neurons and were collected and pooled (Figure 2.2). In order to dilute out the gradient material the cell slurry was mixed with 10ml HABG and centrifuged at 1,100 r.p.m for two minutes at 22°C. The supernatant was discarded and the cell pellet was resuspended in 10ml of HABG. The cell

suspension was centrifuged at 1,100 r.p.m for two minutes at 22°C. The supernatant was removed and the cell pellet was resuspended in 1ml of Neurobasal A™ (Invitrogen) culture media (Neurobasal A™ supplemented with 1X B27™, 35 mM D-Glucose, 0.4 mM L-glutamine, and 1%P/S) for cell counting by Trypan Blue exclusion using a haemocytometer. The cells were resuspended in the appropriate volume of culture media and plated at a density of 10, 000 cells/well of an eight chambered glass slide (NUNC) or a density of 15, 000 cells/ glass coverslip of a 24 well plate. The glass chambered slides and the coverslips were pre-coated for 24 hours with laminin (500 µg/ml) and poly-L-Lysine (5 mg/ml). After being plated down for 30 minutes the cells were washed twice with 200ul of 37°C HABG in order to remove contaminating oligodendrocytes. The washes were removed and replaced with the appropriate media depending on the experiment: i) base culture media, ii) base culture media + NT3 (25 ng/ml, Millipore) or iii) base culture media + NT3 + CNTF (25ng/ml, Sigma). One day following plating the appropriate cell culture medium was refreshed and some cells were treated with an HDAC inhibitor (either Trichostatin A 10 nM, Sigma; or Tubastatin A 15 nM, BioVision), all cells were allowed to grow for two more days (Table 2.1). In all conditions cells were grown *in vitro* for three days before immunocytochemistry was performed.

2.3 Immunocytochemistry

Cells were fixed for immunocytochemistry in 4% paraformaldehyde (PFA) for 15 minutes, followed by three, five minute washes in PBS. Cells were then permeabilized in 0.01% Triton X-100™ for 30 minutes, rinsed in PBS three times for five minutes, blocked in 4% normal goat serum (NGS, Sigma) in PBS for 20 minutes and then incubated in

primary antibody (Table 2.2) overnight at 4°C in 2% NGS. Cells were then washed three times for five minutes in PBS and incubated in secondary antibodies in 2% NGS for one hour at room temperature. Fluorescently labelled secondary antibodies, used at a dilution of 1:1000, were Molecular Probes Alexa 488 and Alexa 594, raised in donkey or goat. Wells or coverslips were washed twice for five minutes in PBS and then nuclei were counter-stained with 4'6-diaminopyridine-2- phenylindole (DAPI; 1:10 000, Sigma) for five minutes at room temperature. Cells were washed twice for five minutes in PBS and then mounted using DABCO (Sigma).

Exceptions: Cells probed for nuclear markers were subjected to antigen retrieval for three minutes in cold neat methanol and then washed for five minutes in PBS in between the fixing and the permeabilization steps outlined above.

2.4 Image Analysis and Quantification

2.4.1 Image acquisition

All images were visualized with an Axioplan 2 Imaging microscope (Zeiss, Jena GER) using a AxioCam HRm camera (Zeiss, Jena GER) and were compiled using Adobe Photoshop 10.0. To characterize the cell populations in the corticospinal neurite culture images were collected from coverslips or chambered slides at 10X magnification.

2.4.2 Neuron and corticospinal neuron counting using the Cellomics automated microscope

For automated image analysis, images of neurons were acquired using the Cellomics VTI Array Scanner automated microscope; using DAPI to identify nuclei, NST fluorescence to identify neurons and GFP fluorescence to identify the YFP-positive CST neurons. The Target Activation v3.5 paradigm was used in order to establish the percentage of NST positive neurons and YFP positive corticospinal neurons in each condition 45 fields of view were captured per well and the percent responder for NST and GFP were recorded in addition to the overall number of DAPI positive nuclei in each field of view. Bright pyknotic DAPI-positive nuclei or nuclei fragments were excluded from the count by setting the threshold for “average intensity” and cell size appropriately (Figure 2.3). Four experiments were done with three replicate wells and one experiment was done with duplicate wells. At least three independent replicate experiments were performed per condition. Data were exported to Microsoft Excel for further analysis.

2.4.3 Montaging and quantification of neurite length, branching and the number of primary neurites from individual neurons

Triple-fluorescent 20x images of YFP-expressing neurons immunolabeled with anti-NST and labeled with DAPI were captured using the Zeiss fluorescent microscope as mentioned above. The intensity of the YFP signal after 3DIV is faint so we used an anti-GFP antibody which binds to YFP positive neurons in order to increase signal intensity. For quantification of neurite outgrowth from single cells an average of 22 individual YFP positive CST neurons were captured at 20X magnification per condition. Images were

photomerged in Adobe Photoshop 10.0 and thresholded to a common level using ImageJ in order to convert images into a binary format. Cell bodies were removed from the thresholded image. ImageJ was then used to skeletonize the neurites, reducing them to a single pixel width and producing a continuous skeleton of neurite outgrowth representing the entire neurite carpet (Figure 2.4). The total number of pixels were converted to micron values based on the magnification of the original image. The number of primary neurites ($\geq 10\mu\text{m}$) and branch points were counted manually on 40X magnification at the time of image capture. Four experiments were performed with three replicate wells and one experiment was done with duplicate wells. At least three independent replicate experiments were performed per condition. Data were recorded and processed using Microsoft Excel.

2.4.4 Quantification of total CST neurite carpet outgrowth per field of view

Triple-fluorescent 20x images of YFP-expressing neurons immunolabeled with anti-NST and DAPI were captured using the Zeiss fluorescent microscope as mentioned above. Fifteen non-overlapping images containing GFP positive neurite outgrowth were captured per well at 20X magnification. Images were imported into ImageJ and thresholded after which the debris and the cell bodies were removed from the image. ImageJ was then used to skeletonize images as mentioned above (Figure 2.5). The total number of pixels was converted to micron values based on the magnification of the original image. Four experiments were performed with three replicate wells and one experiment was done with duplicate wells. At least three independent replicate experiments were performed per condition. Data were recorded and processed using Microsoft Excel.

2.4.5 *Statistical analysis*

Upon consultation with a post-doc in the statistics department, T- tests were used to compare the means between two groups with equal variance. However, a one way ANOVA with a post test such as the Tukey or Bonferroni correction would have also been appropriate. Data were entered into Microsoft Excel. Graphical data was created using GraphPad Prism V5 and is presented with error bars representing standard error of the mean.

Table 2.1 Experimental Conditions: Growth Factors and HDAC Inhibitors

Condition	Growth Factor	Drug Treatment
1a Baseline	No	No
1b	No	10 nM TSA
1c	No	15 nM Tubastatin A
2a	NT3	No
2b	NT3	10 nM TSA
2c	NT3	15 nM Tubastatin A
3a	NT3+CNTF	No
3b	NT3+CNTF	10 nM TSA
3c	NT3+CNTF	15 nM Tubastatin A

TABLE 2.2 Antibodies Used for Immunocytochemical Assessments

Antigen	Supplier	Dilution	Purpose
Mouse anti- NST	Covance	1:500	Identification of neurons and quantification of neurite outgrowth
Chicken anti-GFP	Aves	1:1000	Increases the intensity of the YFP ⁺ CST neurons Identification of CST neurons and quantification of CST neurite outgrowth
Rat anti-CTIP2	Abcam	1:500	Identification of deep layer cortical(corticospinal) neurons
Mouse anti- Otx1	Developmental Studies Hybridoma Bank	1:100	Identification of deep layer cortical(corticospinal) neurons
Rabbit anti-GFAP	Dako Cytomation	1:750	Identification of astrocytes
Mouse anti-CNPase	Abcam	1:100	Identification of oligodendrocytes

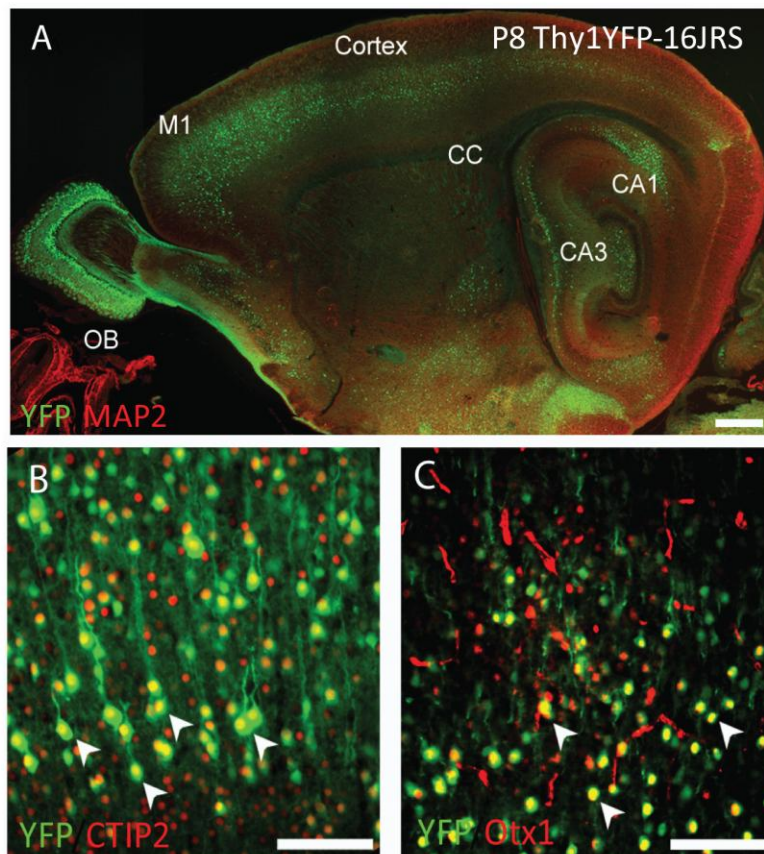


Figure 2.1 YFP Expression in the Postnatal Day Eight Thy1 YFP-16JRS Mouse Identifies a Population Layer Five Projection Neurons

(Adapted from Richter and Roskams, 2009) Endogenous YFP (green) expression in a P8 Thy1-16JRS mouse is found in many brain regions including projection neurons of the olfactory bulb (OB), CA1 and CA3 regions of the hippocampus, and in deep layer 5 cortical neurons in the primary motor cortex (M1). Most YFP-expressing neurons are also positive for (B) Ctip2 (red) and (C) Otx1 (red) (arrowheads). Scale bars 100 μ m.

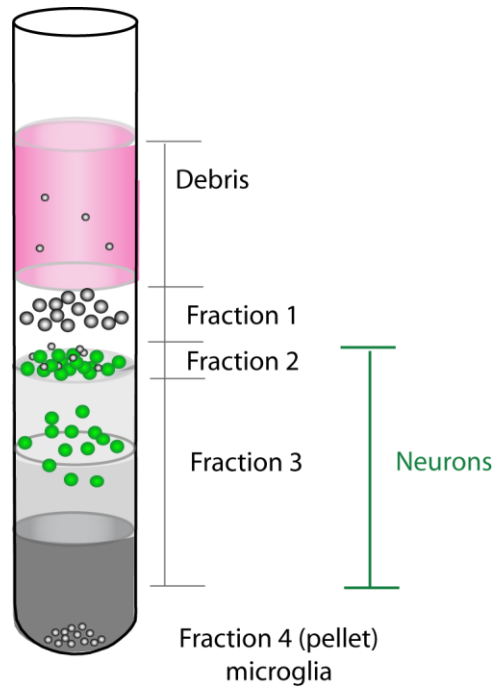


Figure 2.2 The Optiprep™ Density Gradient Separates Cells Based on Density and Allows for the Isolation of a Neuronal Fraction

(Figure adapted from Brewer and Torricelli, 2007) Fraction one contains oligodendrocytes.

Fraction two contains neurons and other cell types. Fraction three contains mostly neurons and fraction four contains a microglial pellet. Fractions two and three were pooled and cultured.

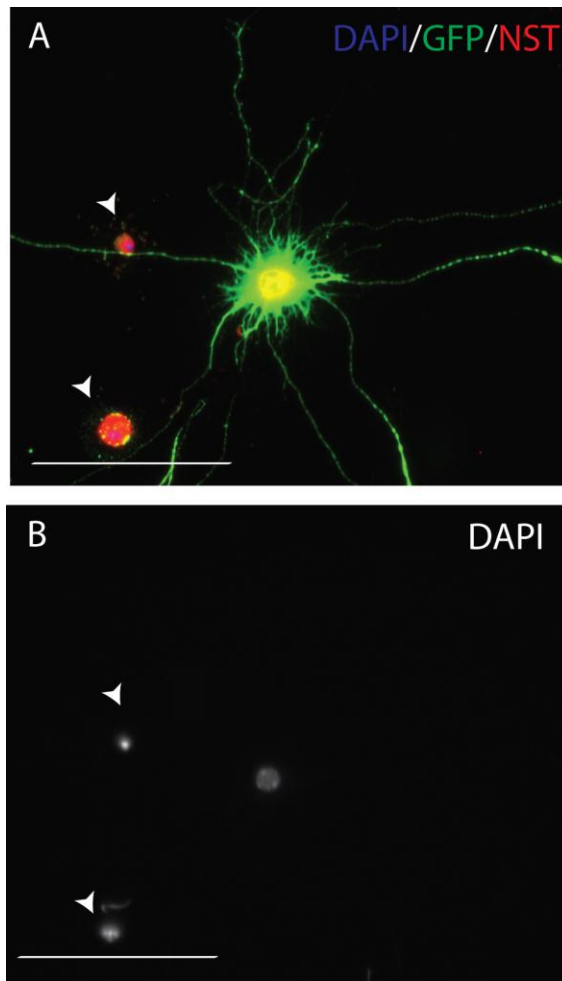


Figure 2.3 DAPI Positive Pyknotic Nuclei and Cell Fragments Were Removed From Cellomics Analysis

YFP expressing corticospinal neuron (green) surrounded by two decaying cells (red, green speckles) (arrowheads) (A). Representation of bright pyknotic nuclei that would have been excluded from cellomics analysis based on intensity and size (B) (arrowheads). Scale bars are 40 μm .

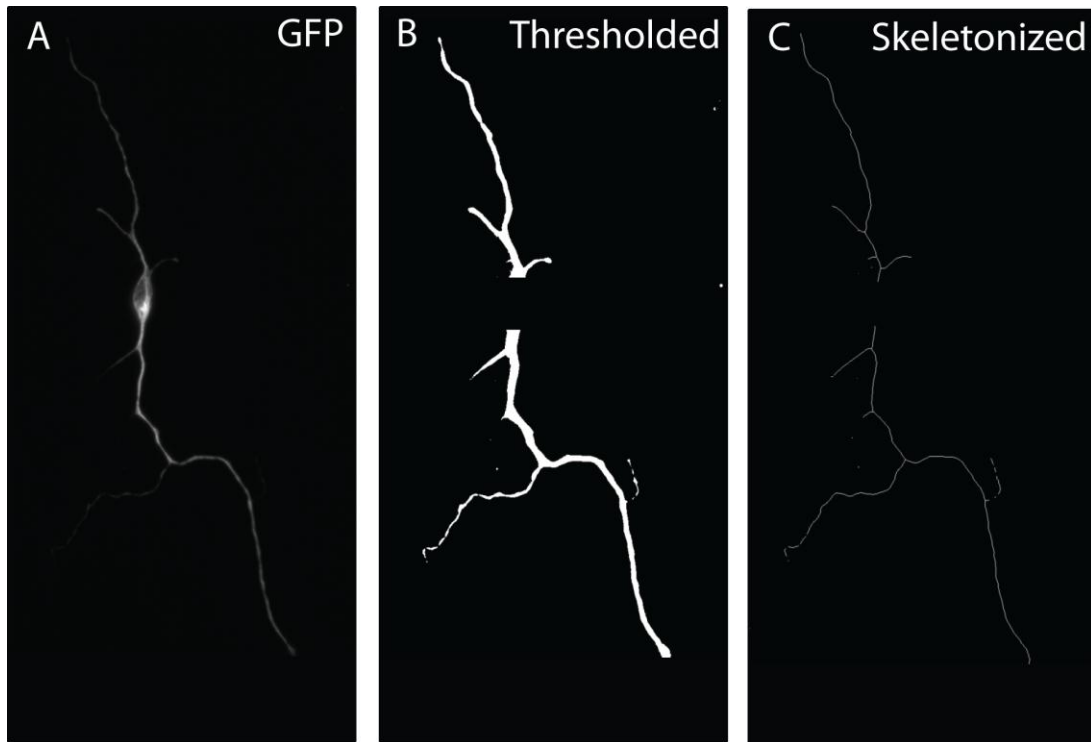


Figure 2.4 Single Cell Outgrowth of Corticospinal Neurons can be Measured by ImageJ Skeletonization

For quantification of neurite outgrowth from single cells the total arborization of individual CST neurons was captured at 20X magnification (A). Images were photomerged in Adobe Photoshop 10.0 and thresholded to a common level using ImageJ in order to convert images into a binary format (B). Cell bodies were removed from the thresholded image. ImageJ was then used to skeletonize the neurites, reducing them to a single pixel width and producing a continuous skeleton of neurite outgrowth representing the entire neurite carpet (C). The total number pixels were converted to micron values based on the magnification of the original image.

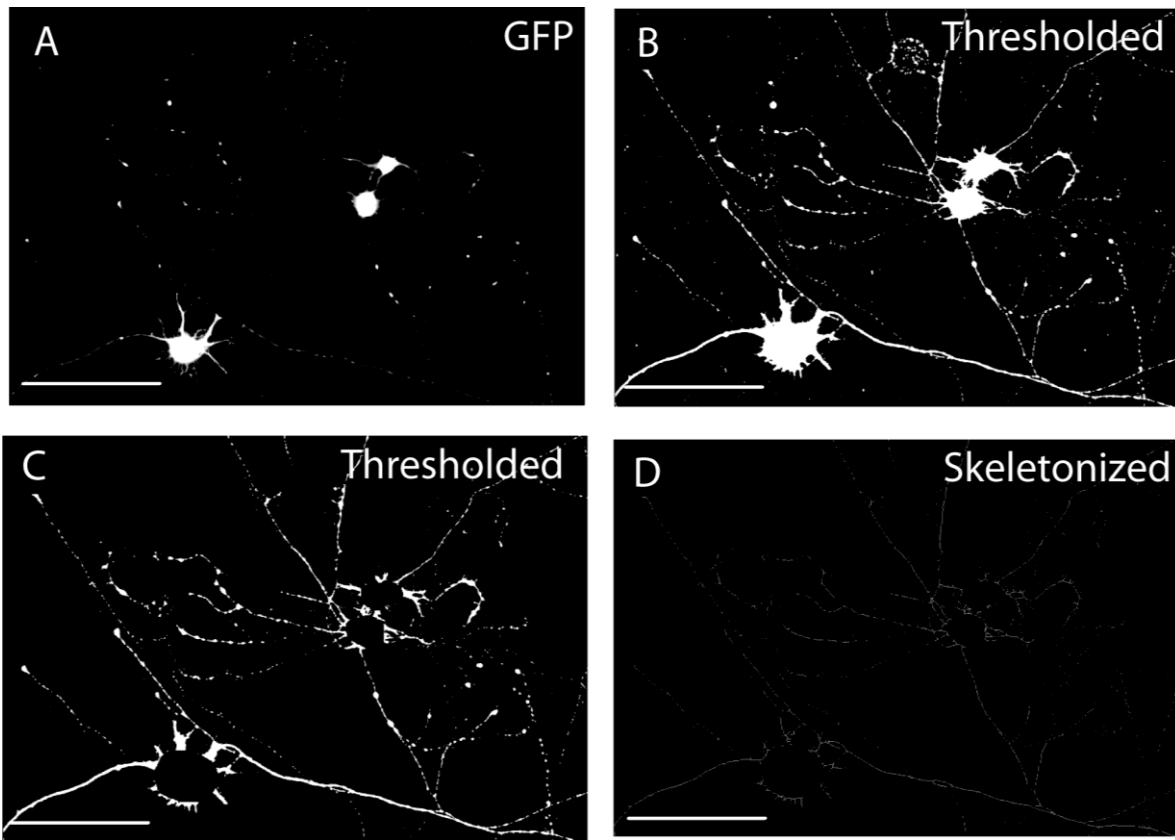


Figure 2.5 Total Neurite Outgrowth of CST Neurons in a Field of View can be Measured by Imagej Skeletonization

For quantification of neurite outgrowth from a field of view the total neurite carpet of CST neurons in a 20X field of view was captured (A). Images were thresholded to a common level using ImageJ in order to convert images into a binary format (B). Cell bodies were removed from the thresholded image (C). ImageJ was then used to skeletonize the neurites, reducing them to a single pixel width and producing a continuous skeleton of neurite outgrowth representing the entire neurite carpet (D). The total number pixels were converted to micron values based on the magnification of the original image. Scale bars are 40 μm .

CHAPTER 3 : RESULTS

3.1 YFP Expression in P8 Thy1-YFP-16JRS Mice Demarcates a Population of Corticospinal Neurons *in vivo*, which is Maintained *in vitro*

In order to investigate whether HDAC inhibitors can promote outgrowth of corticospinal tract neurons *in vitro*, we cultured neurons from the Thy1-YFP-16JRS transgenic mouse, which can provide a means for detecting CST neurons *in vivo* and *in vitro* (Richter and Roskams, 2009). Previous work in the lab examined YFP expression *in vivo* at P8 and found that YFP is vibrant in the soma of layer 5 cortical neurons, as well as in subsets of neurons in the cerebellum, hippocampus and in the mitral cells of the olfactory bulb (Figure 3.1) (Richter and Roskams, 2009). *In vivo*, YFP is absent from the upper layers of the cortex. *In vitro*, after 3DIV the cell bodies of YFP positive neurons were shown to express the CST transcription factor Ctip2, and deep layer cortical transcription factor, Otx1 (Figure 3.1). Both transcription factors co-label with the DNA stain, DAPI in the nucleus (Figure 3.1). The YFP positive neurons also retain the hallmark morphology of CST neurons: pyramidal shaped cell bodies with tufted apical and basal dendrites. In order to identify the other types of cells in the culture system, immunocytochemistry was performed at 3DIV for the following antigens: neuron specific tubulin (NST or β III tubulin) for neurons, glial fibrillary acid protein (GFAP) for astrocytes, CNPase for oligodendrocytes and Ib4 for microglia. In addition to a subset YFP positive CST neurons, the culture contained other YFP negative/ NST positive neurons, microglia, oligodendrocytes and astrocytes (Figure 3.2). In order to ensure that the culturing method yielded similar numbers of total neurons and YFP positive neurons in every experiment we recorded the percentages

of NST positive and GFP positive cells across all conditions and experiments. The percentage of total NST positive neurons in culture typically ranged from 20-30 percent with the average being 23 percent (n = 3-5) (Figure 3.2). The percentage of YFP positive CST neurons in culture ranged from 5-13 percent with the average being nine percent (n = 3-5) (Figure 3.2).

3.2 Establishing Experimental Conditions with NT3, CNTF and HDAC Inhibitors

Initial experiments were performed in the presence of NT3 and CNTF, neurotrophins which have been shown to have neuroprotective effects on CST neurons (Giehl, 2001). The addition of these two growth factors to the culture media dramatically increased neurite outgrowth. In order to ensure that the HDAC inhibitors applied to the culture had an autonomous effect on outgrowth and were not just working with NT3 + CNTF in an additive manner, we investigated CST neuron outgrowth in baseline media, in the presence of NT3 alone, and in the presence of both NT3 and CNTF. Two HDAC inhibitors, TSA and Trichostatin A, were of particular interest as they can increase outgrowth of embryonic cortical neurons *in vitro* (Rivieccio et al., 2009). In the current study we wished to investigate whether more mature P8 CST neurons, which have already established synaptic connections with their targets, would exhibit increased neurite outgrowth in response to TSA or Tubastatin A. In order to establish an effective inhibitor concentration for treatment, initial dose response studies were performed in the presence of NT3+CNTF. Preliminary results showed that TSA increased neurite outgrowth when applied at 10 nM and 20 nM, but began to decrease neurite outgrowth when applied at a concentration of 50 nM (Figure 3.3). Tubastatin A was applied to the culture in the following concentrations:

15 nM, 100 nM and 500 nM. The highest increase in neurite outgrowth was observed in the 15 nM condition (Figure 3.4). Based on the initial outgrowth trends, treatment of 10 nM TSA or 15 nM Tubastatin A were used for all further experiments.

3.3 In the Presence of NT3 and CNTF, Tubastatin A and TSA Increase the Number of NST Positive and YFP Positive Neurons Respectively

In order to investigate whether 10 nM TSA and 15 nM Tubastatin A enhance survival of CST neurons we recorded the total number of DAPI positive cells and the percentages of NST positive and YFP expressing neurons in each treatment condition (see Table 2.2 for all experimental conditions). The data from each condition were represented graphically as a percentage of the baseline condition (media contained no NT3, CNTF or inhibitor).

Application of 10 nM TSA to baseline media significantly increased number of DAPI positive cells ($n = 4$, $p = 0.0019$) (Figure 3.3). The total number of DAPI positive cells also significantly increased compared to baseline when treated with 10 nM TSA ($n = 3$, $p = 0.0111$) or 15 nM Tubastatin A ($n = 3$, $p = 0.0046$) in the presence of NT3+CNTF (Figure 3.3)(See Appendix 5.1 for raw numbers of DAPI positive cells).

This suggests that the ability of TSA to increase the total number of cells in culture is independent of growth factor application. TSA and Tubastatin A also appear to work in concert with NT3+CNTF to increase the number of surviving cells over the baseline treatment.

In the presence of NT3 and CNTF, application of Tubastatin A significantly increased the number of NST positive neurons ($n = 3$ separate experiments, $p = 0.0101$) (Figure 3.4) (See Appendix 5.2 for raw numbers of NST positive cells in each experiment)

and application of TSA significantly increased the number of YFP positive corticospinal tract neurons ($n = 3$, $p = 0.0468$) in culture compared to baseline (Figure 3.5) (See Appendix 5.3 for raw numbers of YFP positive cells in each experiment). The addition of NT3 or NT3+CNTF to the culture did not significantly alter the number of surviving DAPI positive cells, NST positive neurons or YFP positive corticospinal neurons. This suggests that the combination of NT3+CNTF with either TSA or Tubastatin A works in concert to increase the number of YFP or NST positive cells respectively.

3.4 Corticospinal Neuron Outgrowth, Branching and Primary Neurites in Response to Treatment with HDAC Inhibitors TSA and Tubastatin A

There was a significant increase in the number of primary neurites per YFP positive neuron after TSA treatment in the absence of NT3+CNTF compared to the baseline condition ($n= 4$, $p = 0.0155$) (Figure 3.8). In all other conditions the number of YFP positive primary neurites per neuron was fairly consistent and the average ranged from three-five neurites per neuron (Figure 3.8)(See Appendix 5.4 for the numbers of primary neurites per YFP positive neuron in each experiment). In the absence of NT3+CNTF, both TSA ($n = 4$, $p = 0.0305$) and Tubastatin A ($n = 3$, $p = 0.0431$) significantly promoted neurite branching in YFP positive CST neurons (Figure 3.9). There was also a significant increase in the number of branch points in the NT3+CNTF+Tubastatin A condition over baseline (Figure 3.7)(See Appendix 5.5 for the numbers of branch points per YFP positive neuron in each experiment).

All conditions, except NT3 alone, showed a significant increase in YFP positive neurite outgrowth per neuron, compared to the baseline condition (Figure 3.10). Both TSA

and Tubastatin A significantly increased the amount of YFP positive neurite outgrowth compared to baseline, in the absence of NT3 or CNTF (TSA, n=4, p= 1.282*10⁻⁵; Tubastatin A, n=3, p=0.0171), in the presence of NT3 (TSA, n=4, p=0.0011; Tubastatin A, n=3, p=0.0149) and in the presence of NT3+CNTF (TSA, n=3, p=0.0145; Tubastatin A, n=3, p=0.0123)(Figure 3.10)(See Appendix 5.6 for average neurite length (µm)/YFP positive neuron in each experiment). The increase in YFP positive neurite outgrowth after TSA or Tubastatin A treatment in the presence of NT3 and CNTF was significant after performing a t-test or one way ANOVA with Tukey's correction. The increase in neurite outgrowth after application of TSA in the presence of NT3 was significant compared to the NT3 alone condition (n=4, p=0.0117) (Figure 3.10). The extent of corticospinal outgrowth in the NT3+CNTF condition was an average of 220 ± 48 percent higher than the amount of outgrowth present in the baseline condition (no drug treatment or growth factors). In the presence of NT3+CNTF, corticospinal neurite outgrowth increased by 370 ± 88 percent over baseline with TSA treatment and 385 ± 90 percent over baseline after Tubastatin A application. However, the difference between the outgrowth present in the NT3+CNTF condition compared to NT3+CNTF+TSA or NT3+CNTF+TubastatinA was not significant. The abundance of neurite outgrowth in the conditions treated with an inhibitor in the presence of NT3+CNTF made it more difficult to sample the larger than average cells which were heavily intertwined and touching neighbouring cells. While the appropriate number of neurons was sampled in each condition, some of the YFP neurons that were not in direct contact with other neurons were on the fringe of the plating area and were indeed smaller than the average YFP positive neuron in this condition. This resulted in a great deal of variability in neurite outgrowth in the three NT3+CNTF conditions. We adapted our

sampling strategy for quantifying neurite outgrowth to include the total YFP positive neurite outgrowth in a 20x field of view in the three NT3+CNTF conditions in order to see if we could observe a significant increase in outgrowth after treatment of either TSA or Tubastatin A in the presence of NT3+CNTF. Quantification of the total YFP positive neurite outgrowth in a 20x field of view revealed a significant increase in outgrowth compared to baseline in the NT3+CNTF condition (n=3, p=0.0017) as well as in the treatments which paired NT3+CNTF with either TSA (n=3, p=0.0003) or Tubastatin A (n=3, p=0.0001)(Figure 3.11)(See Appendix 5.7 for total YFP positive neurite outgrowth (μm) /20x field of view in each experiment). There was also a significant increase in YFP positive outgrowth observed when treatment with TSA (n=3, p=0.0117) or Tubastatin A (n=3, p=0.0093) was applied in conjunction with NT3+CNTF compared to the NT3+CNTF condition (Figure 3.11). Taken together, both inhibitors are able to promote neurite outgrowth in a manner independent of growth factors but also display increases in outgrowth after applied in conjunction with NT3+CNTF.

Figure 3.1 YFP Positive Neurons Express Markers of Corticospinal Tract Neurons *In Vitro*

YFP positive cells express Ctip2 (A''') and Otx1 (B''') in culture. Arrow heads point to positive nuclei staining for Ctip2 (A''') or Otx1 (B'''). Scale bar is 40 μm in all pictures.

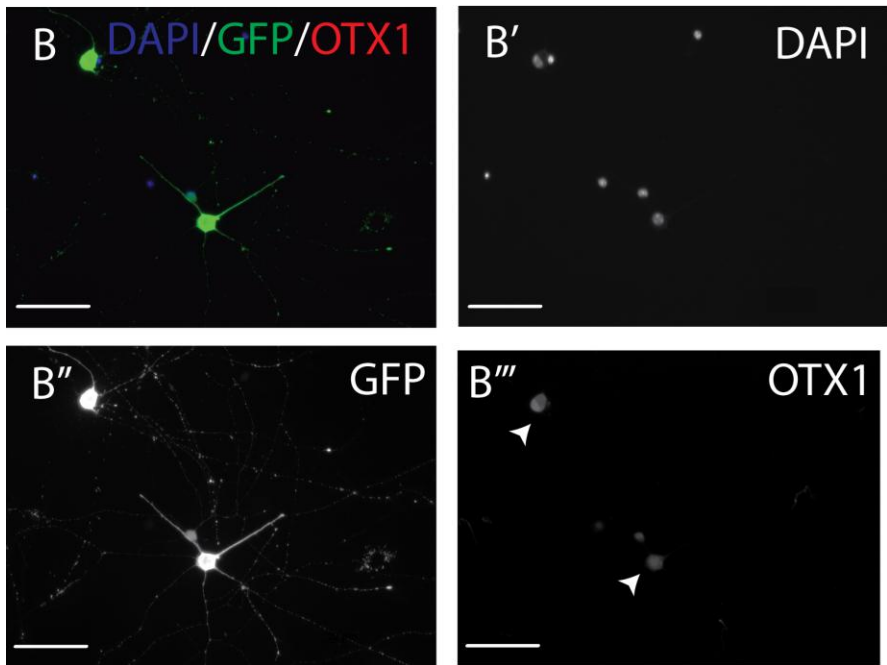
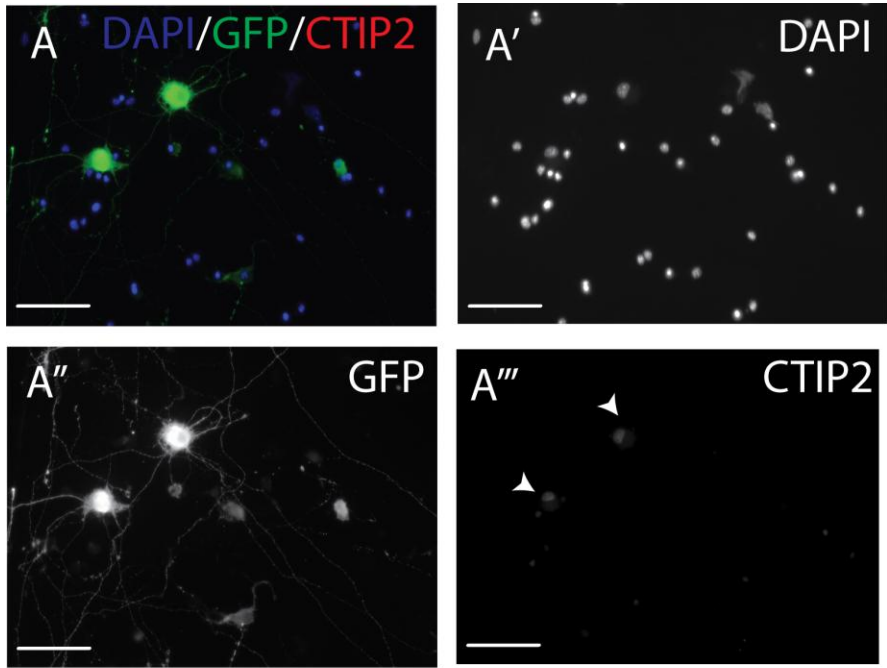
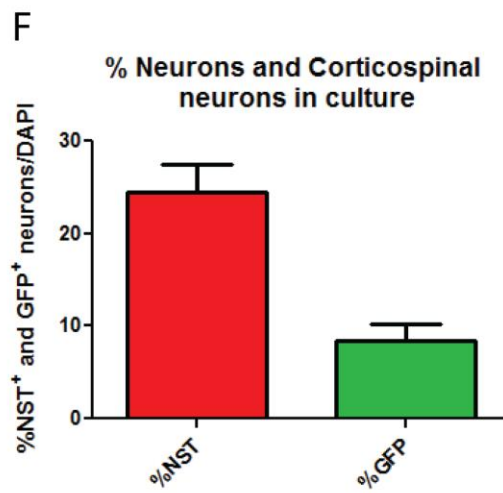
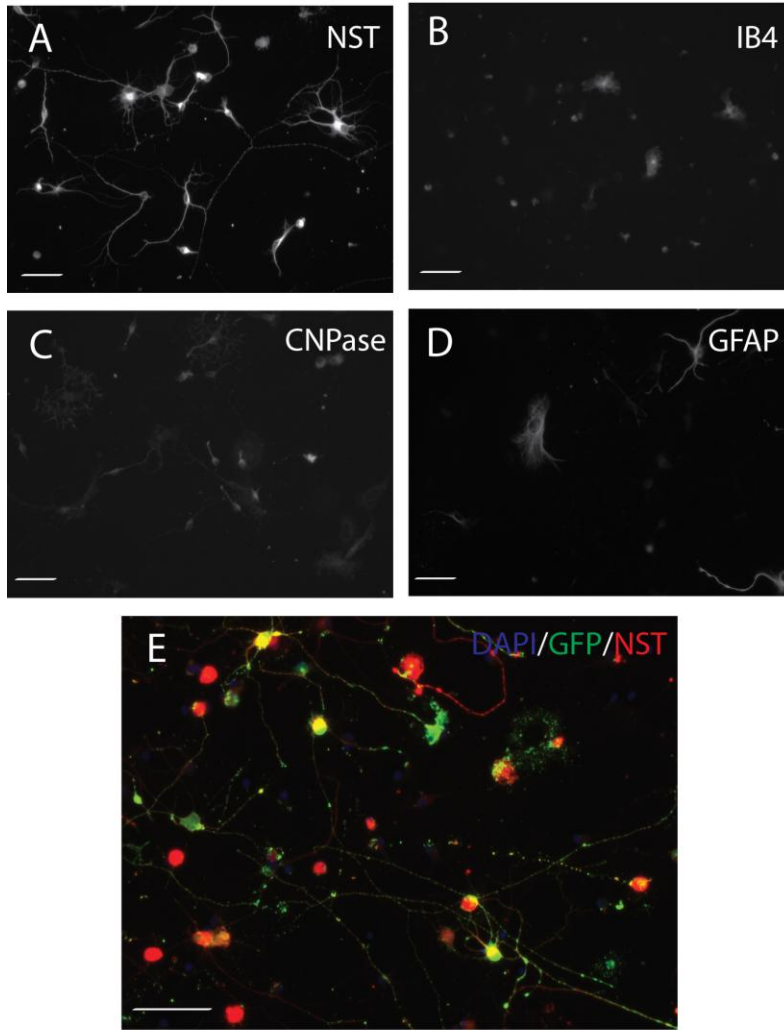


Figure 3.2 The Culture System Contains Various Cell Types and a Consistent Population of NST Positive and YFP Positive Cells Across Experiments

The mixed culture contains neurons (A), microglia (B), oligodendrocytes (C) and astrocytes (D). YFP positive corticospinal neurons are present in the culture (E). (F) The percentage of NST positive-YFP negative cells in each experiment ranges from 22-30 percent and the percentage of YFP positive corticospinal neurons ranges from 5-10 percent. Scale bar is 40 μm in all pictures.



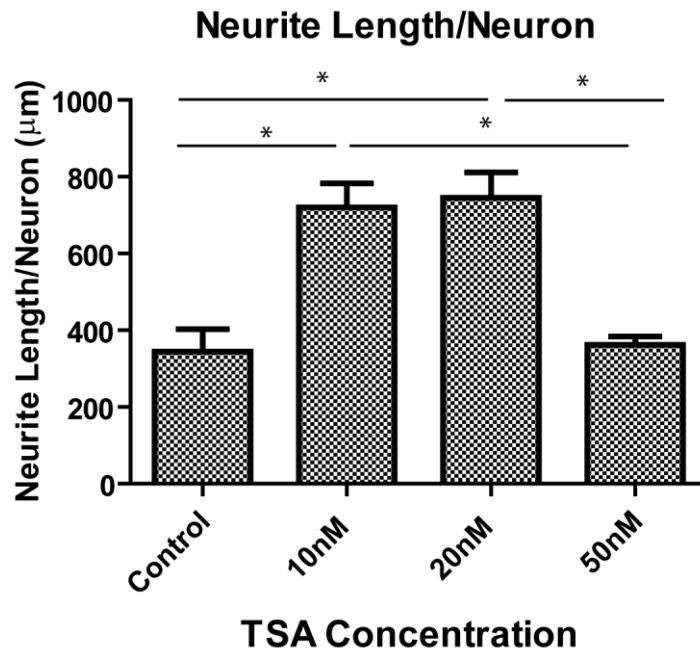


Figure 3.3 Preliminary Data Shows 10 nM TSA Treatment Increases YFP Positive Neurite Outgrowth

There is no significant difference in outgrowth between baseline and 50 nM TSA treatment.

However, application of 10 nM TSA or 20 nM TSA significantly increase the amount of neurite outgrowth compared to the untreated control condition, as denoted by *, $p < 0.05$.

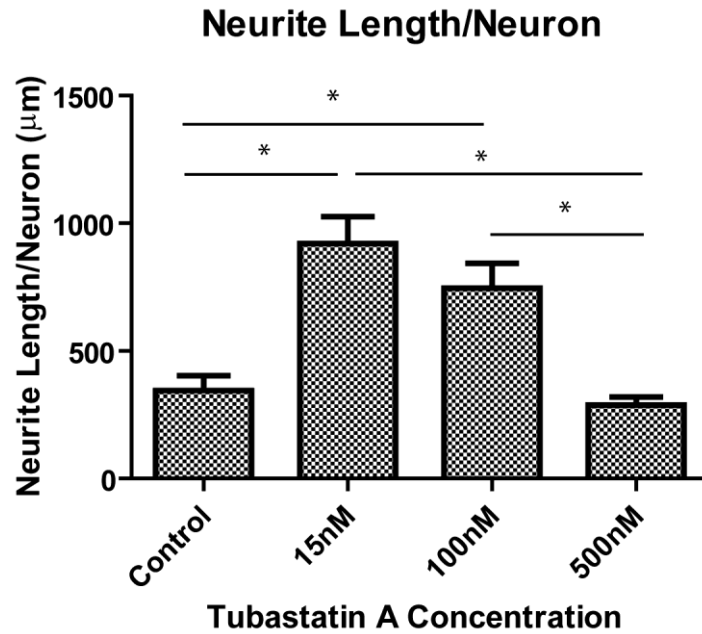


Figure 3.4 Preliminary Data Shows 15 Nm Tubastatin A Increases YFP+ Neurite Outgrowth (μm)

While both 15 nM and 100 nM Tubastatin A increased neurite outgrowth of YFP positive neurites compared to the untreated control, the most outgrowth was present after addition of 15 nM Tubastatin A, as denoted by *, $p < 0.05$.

Figure 3.5 The Total Number of DAPI Positive Cells in Culture Increases in Response to TSA in the Absence of Growth Factors and When TSA or Tubastatin A Treatment is Delivered in the Presence of NT3+CNTF

Representative number of cells after 3DIV in the absence of growth factors (A, A') or in the absence of growth factors with TSA treatment (B, B'). (C) Compared to baseline (no growth factors or drug treatment) TSA increases the number of DAPI positive cells in the absence of growth factors and in the presence of NT3+CNTF. (C) Tubastatin A (referred to Tub A on the graph) significantly increases the number of DAPI positive cells in the presence of NT3+CNTF compared to baseline, as denoted by *, $p < 0.05$. In all inhibitor experiments cells were treated with either 10 nM TSA or 15 nM Tubastatin A. Scale bar is 40 μm in all pictures.

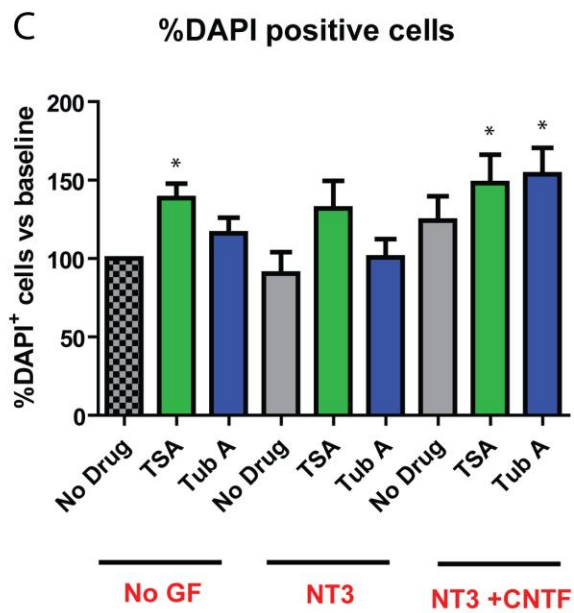
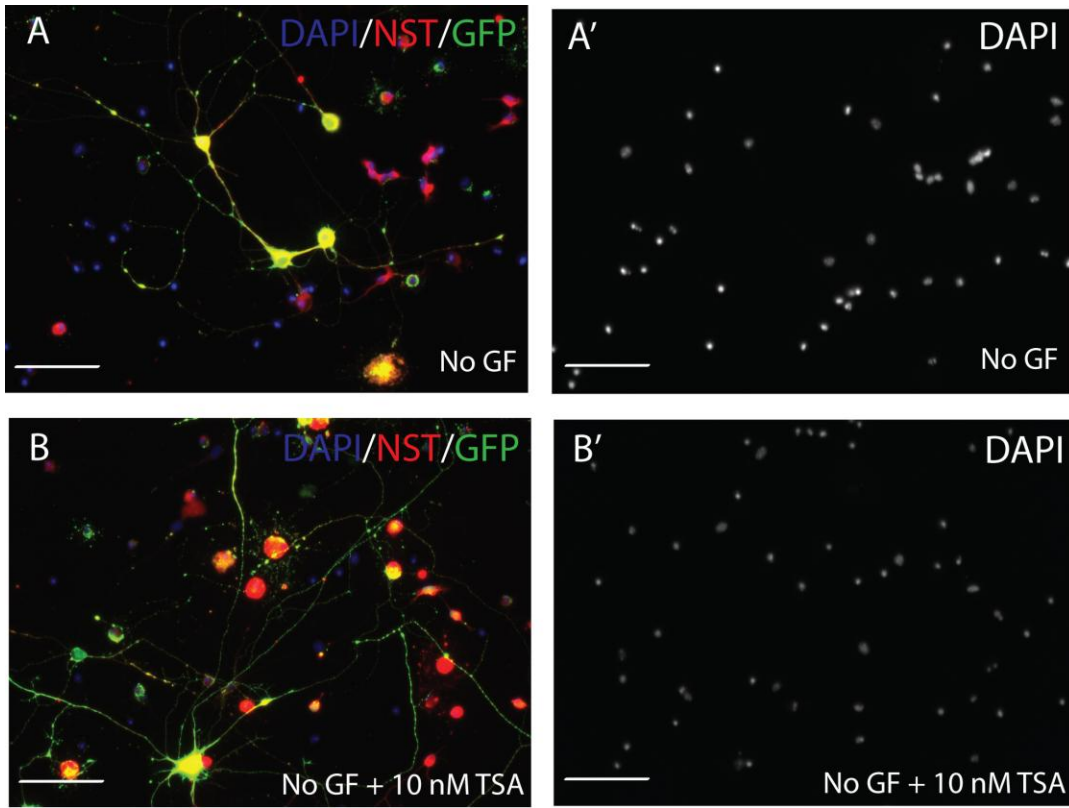


Figure 3.6 The Number of NST Positive Cells was Increased After Treatment With Tubastatin A in the Presence of NT3+CNTF

(A, A') Representative number of NST positive neurons after 3DIV in the baseline condition (absence of both growth factors and drugs). (B, B') Representative number of NST positive neurons after 3DIV in the presence of NT3+CNTF and Tubastatin A (referred to Tub A on the graph). (C) There was a significant increase in the number of NST positive neurons in the presence of NT3+CNTF+Tubastatin compared to baseline as denoted by *, $p < 0.05$. In all inhibitor experiments cells were treated with either 10 nM TSA or 15 nM Tubastatin A. Scale bar is 40 μm in all pictures.

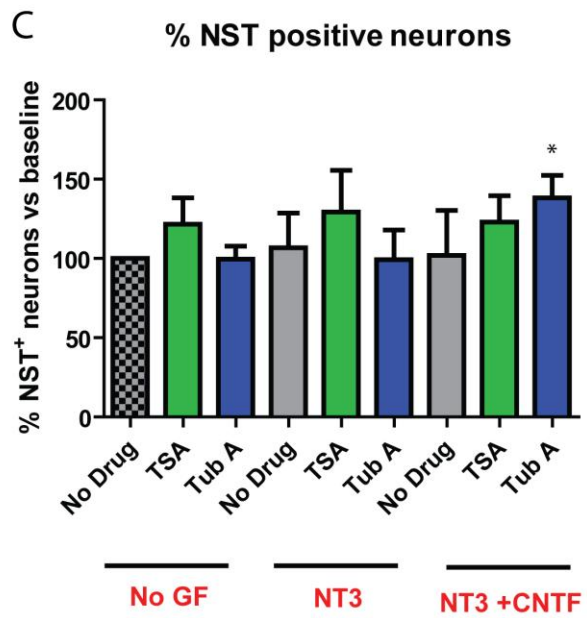
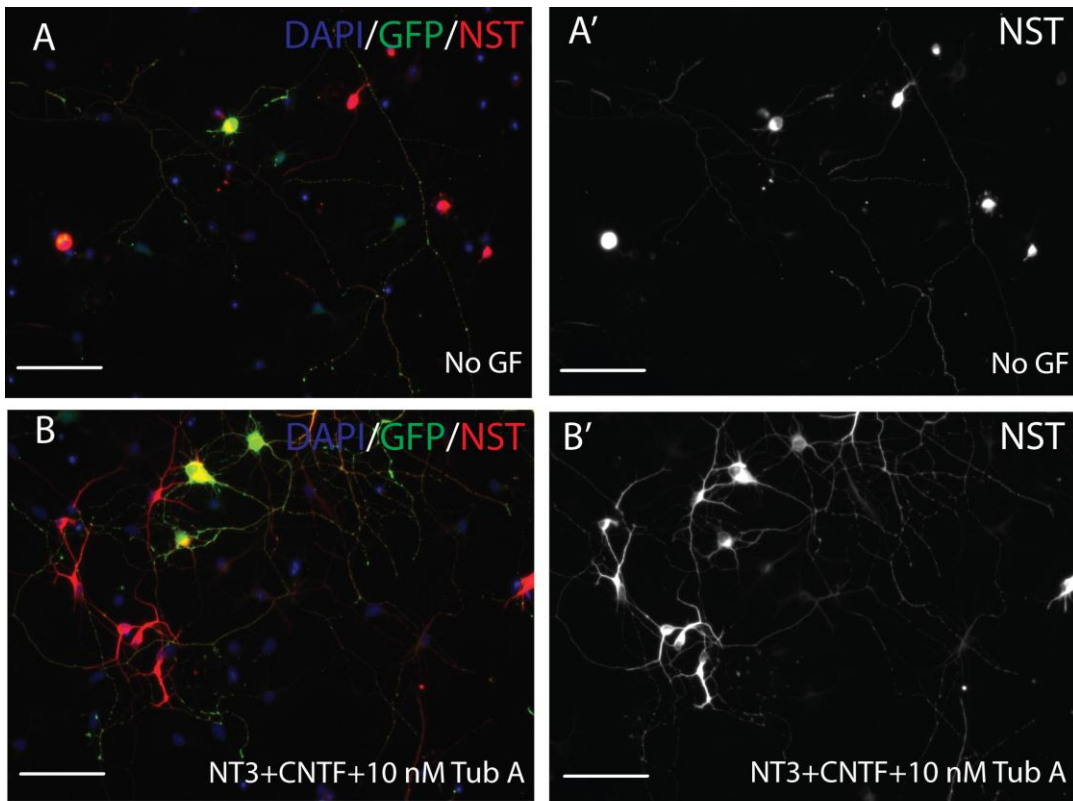
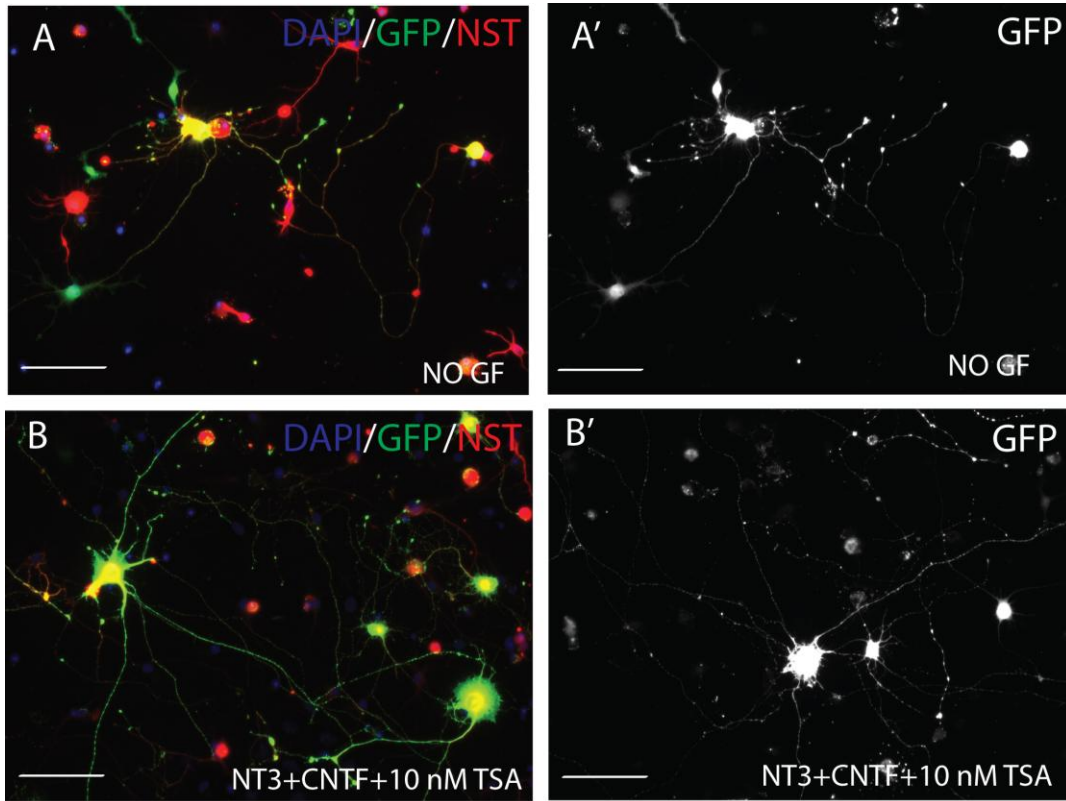


Figure 3.7 The Number of Corticospinal Neurons Increased in Response to Treatment With TSA

(A, A') Representative number of CST neurons after 3DIV in the baseline condition (absence of both growth factors and drugs). (B, B') Representative number of CST neurons after 3DIV in the presence of NT3+CNTF and TSA. (C) There was a significant increase in the number of corticospinal neurons in the presence of NT3+CNTF+TSA compared to baseline as denoted by *, $p < 0.05$. In all inhibitor experiments cells were treated with either 10 nM TSA or 15 nM Tubastatin A. Scale bar is 40 μm in all pictures.



C

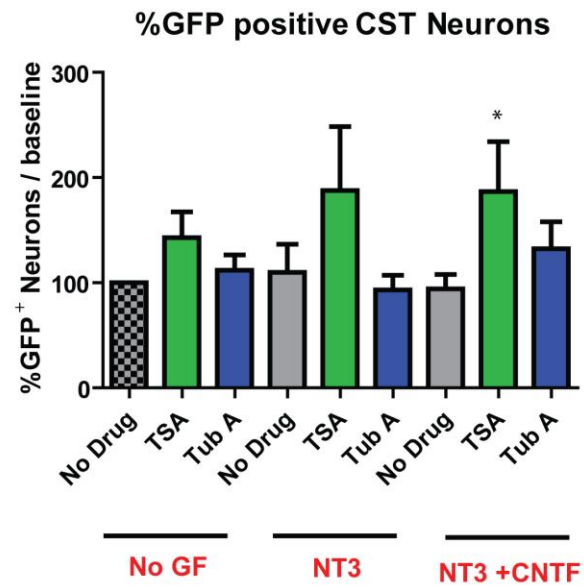


Figure 3.8 Treatment With TSA Increased the Average Number of Primary Neurites of Corticospinal Tract Neurons

The number of primary neurites was variable within each condition, including the no growth factor condition represented here (A,C). The average number of primary neurites per CST neuron was significantly increased after treatment with TSA in the presence of NT3+CNTF compared to baseline (no growth factors or drugs), as represented by *, $p < 0.05$. In all inhibitor experiments cells were treated with either 10 nM TSA or 15 nM Tubastatin A.

Scale bar is 40 μm in all pictures.

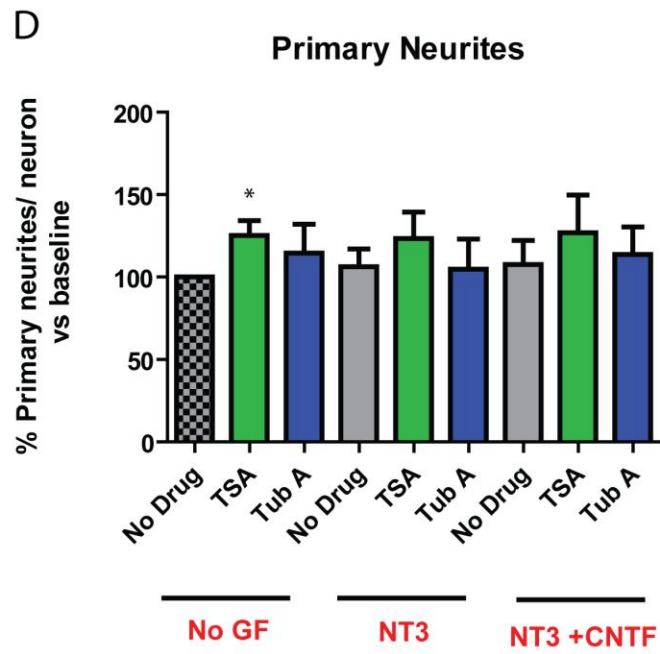
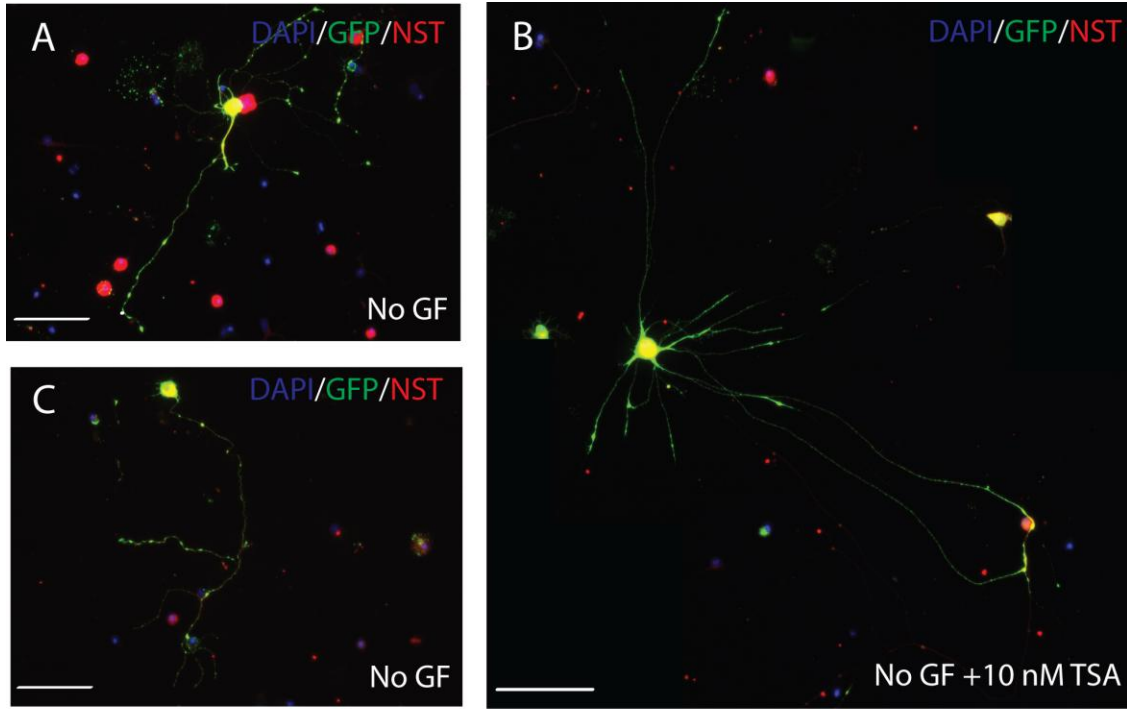


Figure 3.9 Corticospinal Neurite Branching is Increased in Response to TSA and Tubastatin A

The number of branch points was variable within each condition, including the baseline condition (no growth factors or drugs) represented here (A,C). The average number of branch points per CST neuron was significantly increased in response to treatment with TSA or Tubastatin A (referred to Tub A on the graph) in the absence of growth factors, compared to baseline (B). Arrow heads point to examples of branch points. The average number of branch points per CST neuron was also significantly increased with application of Tubastatin A in the presence of NT3+CNTF compared to baseline (D), as represented by *, $p < 0.05$. In all inhibitor experiments cells were treated with either 10 nM TSA or 15 nM Tubastatin A. Scale bar is 40 μm in all pictures.

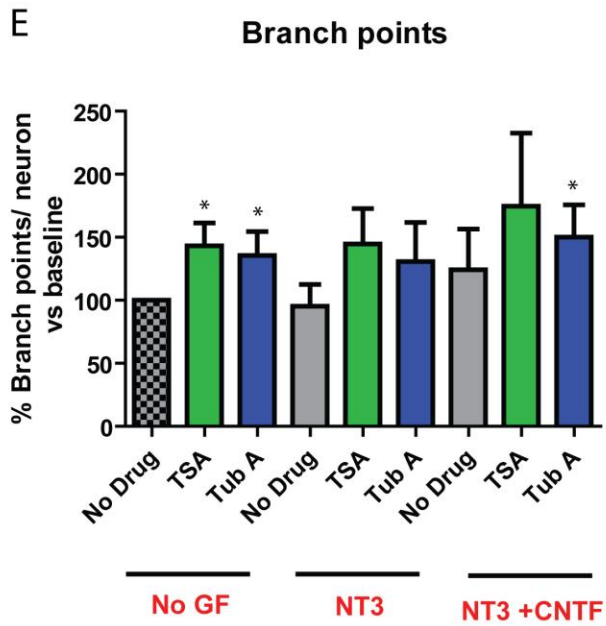
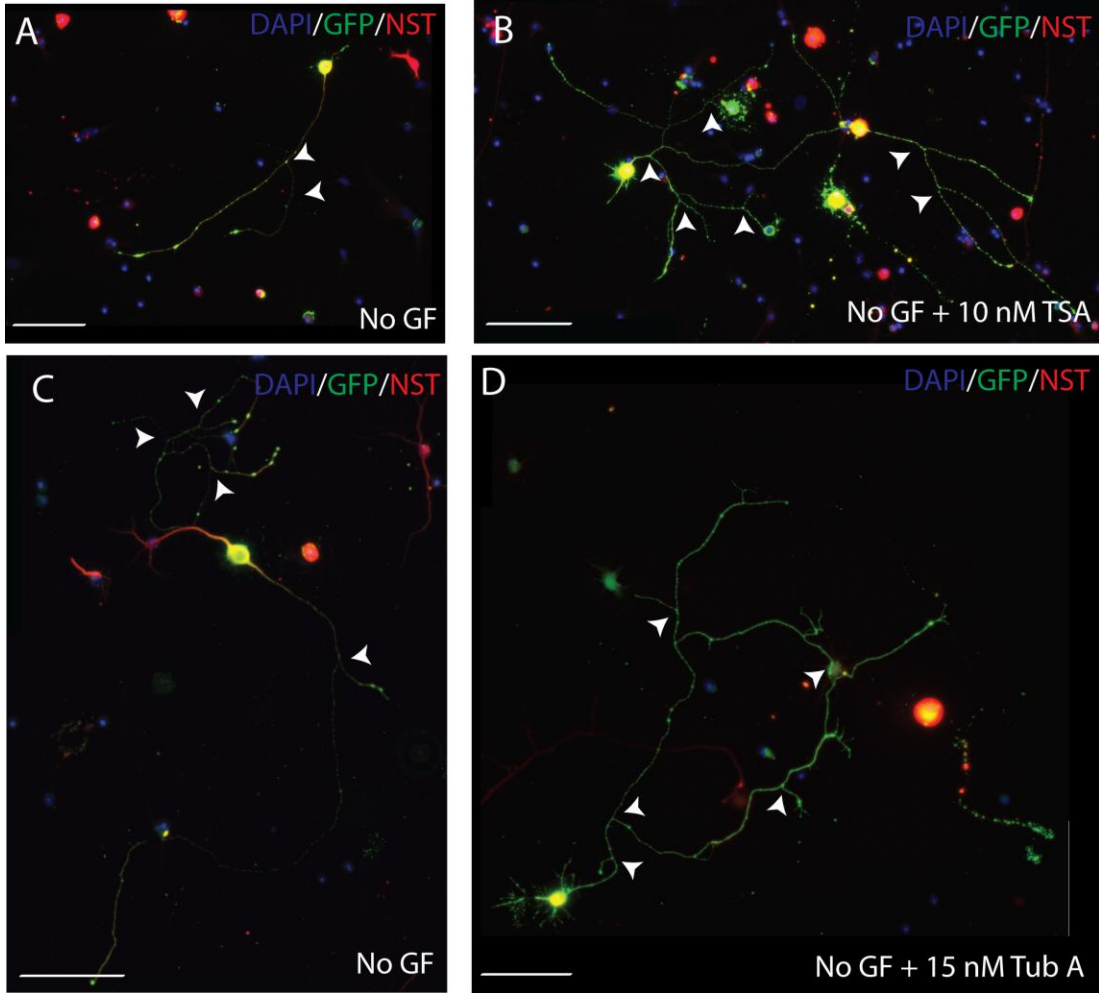


Figure 3.10 Corticospinal Neuron Outgrowth per Cell was Increased in Response to Treatment With TSA or Tubastatin A

Representative corticospinal neurons after 3DIV in the baseline condition (no growth factors or drugs) (A), or after treatment with TSA (B) or Tubastatin A (referred to Tub A on the graph) (C) in the absence of growth factors. Both TSA and Tubastatin A significantly increased corticospinal neurite outgrowth in the absence of growth factors compared to baseline (D). While the NT3 condition did not show an increase in outgrowth in relation to baseline, treatment with NT3+TSA did significantly increase corticospinal outgrowth (D). Treatment with NT3+CNTF alone and after the addition of either TSA or Tubastatin A resulted in an increase in the amount of CST outgrowth compared to baseline, as represented by, * $p < 0.05$ or ** $p < 0.001$. In all inhibitor experiments cells were treated with either 10 nM TSA or 15 nM Tubastatin A. Scale bar is 40 μm in all pictures.

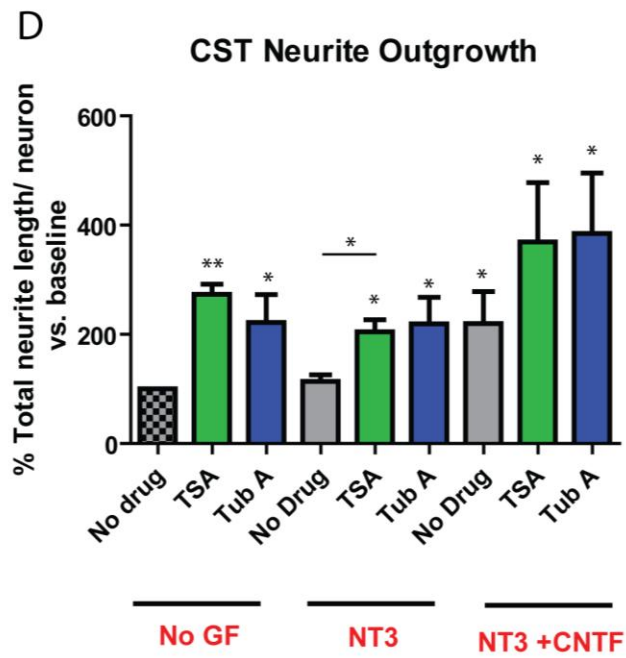
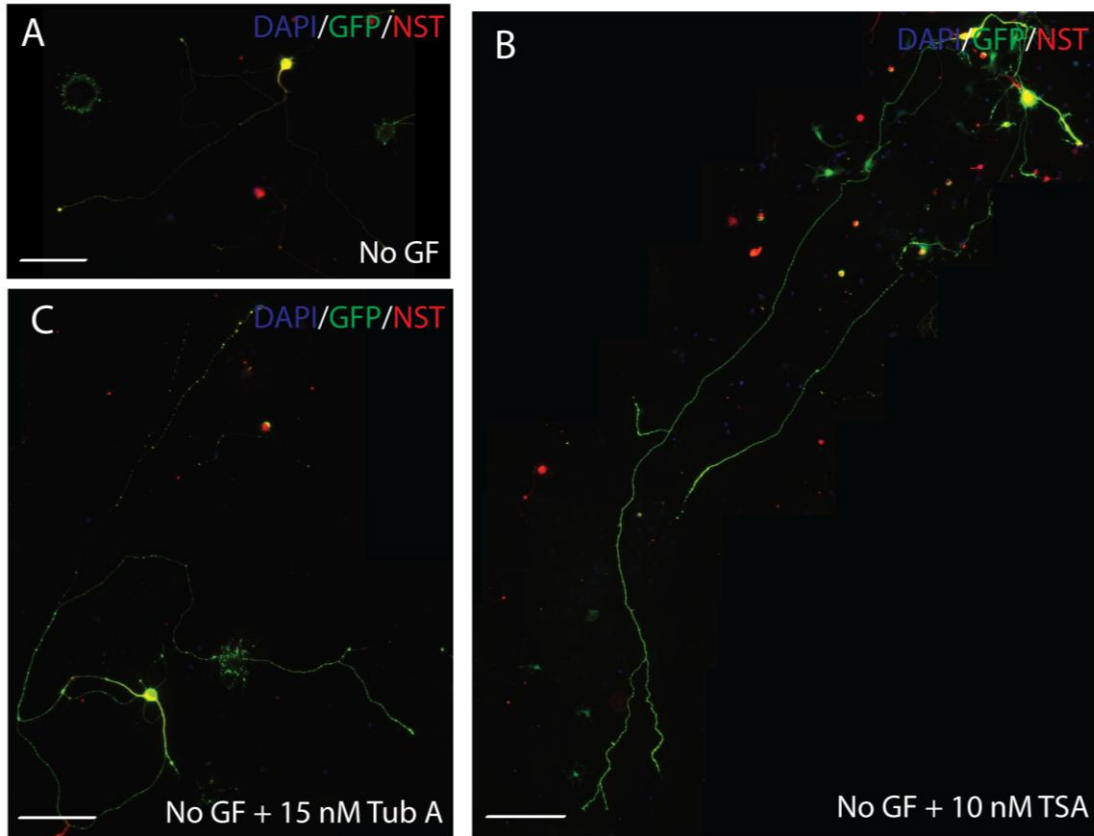
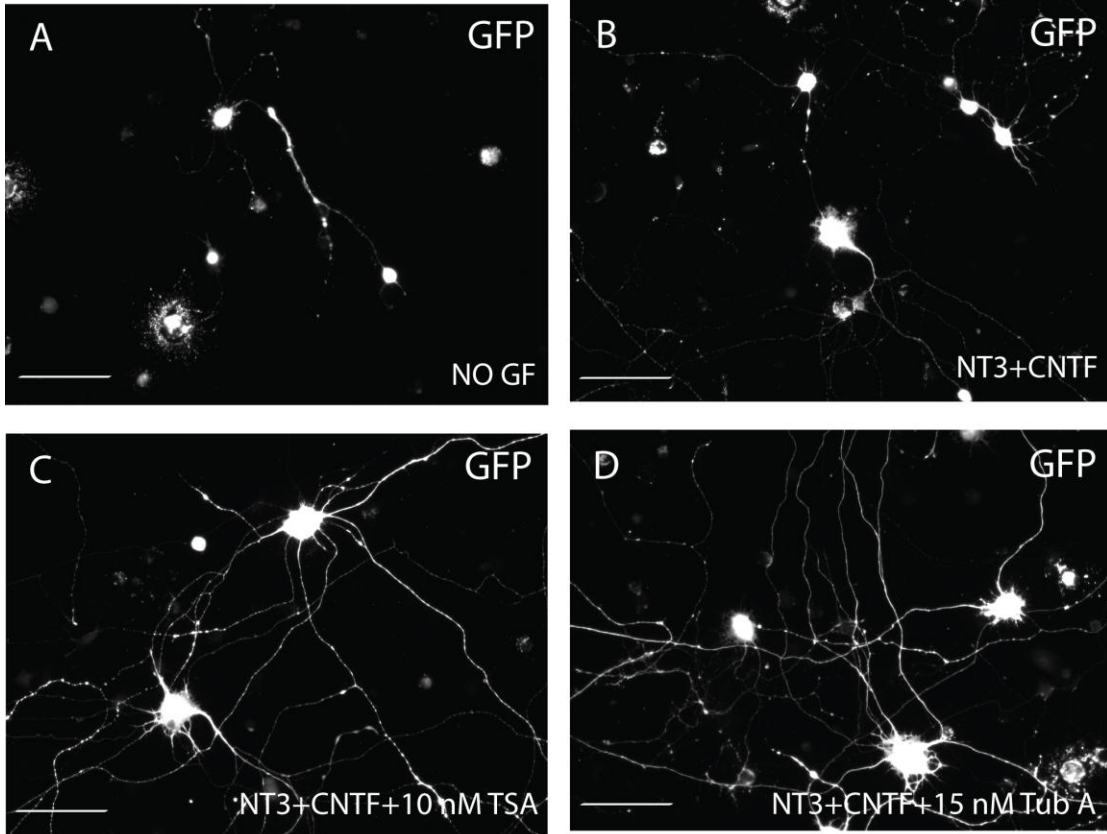
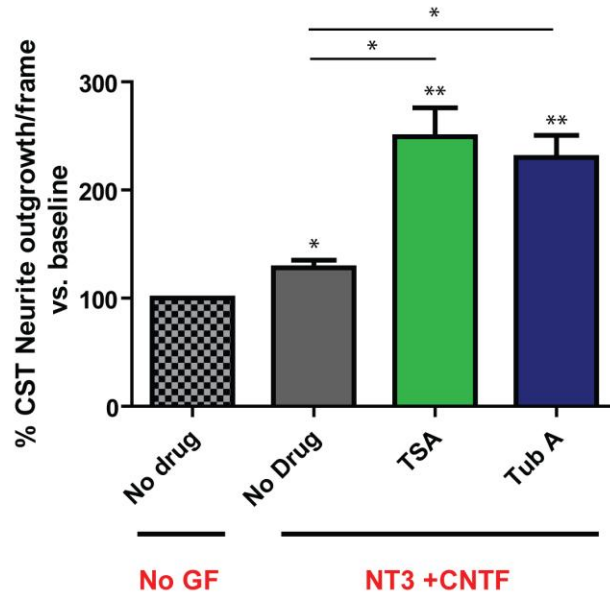


Figure 3.11 Corticospinal Neuron Outgrowth per Field of View Increased in Response to Treatment With TSA or Tubastatin A in the Presence of NT3+CNTF

Representative corticospinal neurite outgrowth in a field of view in the baseline condition (no growth factors or drugs) (A), in the presence of NT3+CNTF alone (B), or after treatment with TSA (C) or Tubastatin A (referred to Tub A on the graph) (D) in the presence of NT3+CNTF. There was a significant increase in neurite outgrowth observed in all conditions relative to baseline (E). Interestingly, CST neurite outgrowth was also significantly higher after the treatment with TSA or Tubastatin A in the presence of NT3+CNTF compared to the NT3+CNTF alone condition; something that was not observed in the neurite outgrowth/single cell method of quantification (E), as represented by *, $p < 0.05$ or **, $p < 0.001$. In all inhibitor experiments cells were treated with either 10 nM TSA or 15 nM Tubastatin A. Scale bar is 40 μm in all pictures.



E CST neurite outgrowth/frame



CHAPTER 4 : DISCUSSION

The current study set out to investigate the effects of HDAC inhibitor treatment on the survival and outgrowth of CST neurons *in vitro* using a combination of high-throughput analysis and careful high resolution morphometry. Our findings are the first to illustrate that HDAC inhibitor treatment can enhance neuron survival, branching and neurite outgrowth of more mature corticospinal neurons *in vitro*.

4.1 YFP Expressing Neurons Exhibit Characteristics of CST Neurons *in vitro*

After 3DIV the YFP positive neurons express the CST specific transcription factors, Ctip2 and Otx1 (Figure 3.1), and display the typical corticospinal neuron morphology—spinous apical and basal dendrites and a large pyramidal shaped soma. The accurate identification of CST neurons *in vitro* based on the aforementioned molecular and morphological characteristics using the Thy-1 YFP mouse has been demonstrated previously (Richter and Roskams, 2009). In addition to CST neurons the culture system contains other neurons which are YFP negative/NST positive as well as astrocytes, oligodendrocytes and occasional microglia (Figure 3.2).

4.2 YFP Expressing CST Neurons Respond to HDAC Inhibition *in vitro*

4.2.1 *HDAC inhibitor treatment increases the number of surviving corticospinal neurons in vitro*

In the presence of both NT3 and CNTF, Tubastatin A significantly increased the number of NST positive neurons (Figure 3.4) and TSA significantly increased the number of YFP positive CST neurons in culture compared to baseline (absence of NT3, CNTF and

inhibitors) (Figure 3.5). However, application of NT3 or NT3+CNTF over a three day time window did not significantly alter the number of surviving DAPI- positive cells, NST-positive neurons or YFP-positive corticospinal neurons. Taken together, this suggests that HDAC treatment is reliant on the presence of NT3+CNTF to increase survival of postnatal cortical neurons maintained in culture short term. HDAC inhibitors have been previously shown to have neuroprotective effects on cortical neurons in models of oxidative stress *in vitro* (Ryu et al., 2003). Ratan and colleagues (2009) demonstrated an increase in embryonic cortical neuron survival after application of TSA or Tubastatin A in a model of oxidative stress and in the presence of inhibitory substrates like MAG, but not in a state of basal media conditions (Rivieccio et al., 2009). These data appear to be the first to demonstrate the acute protective effects of TSA on terminally mature corticospinal neurons *in vitro*.

Multiple mechanisms have been put forward to account for the neuroprotective effects conferred by HDAC inhibitor treatment. Several groups have shown that VPA can induce BDNF expression in both neurons and astrocytes *in vitro* (Wu et al., 2008; Yasuda et al., 2009) and BDNF can promote survival of various neuronal subtypes including injured corticospinal neurons (Klocker et al., 2000; Lu, Blesch, and Tuszynski, 2001; Giehl and Tetzlaff, 1996). Treatment with either VPA or MS-275 activated the promoter of HSP70 in cortical neurons; HSP70 is an important cytoprotective protein that has anti-apoptotic and anti-inflammatory effects (Marinova et al., 2011). Another study illustrated that inhibition of class I and II HDACs using TSA and SAHA blocked Bcl-2-associated X protein (Bax)-dependent apoptosis in postnatal mouse cortical neurons (Uo, Veenstra, and Morrison, 2009). HDAC inhibitors have also been proposed to exert their neuroprotective effects

through transcription dependent means (Langley et al., 2008). Pulse inhibition with TSA resulted in neuroprotection associated with the transcriptional upregulation of a cell cycle inhibitor, p21, in cortical neurons *in vitro* as well as in an *in vivo* model of ischemia (Langley et al., 2008). This cyclin dependent kinase inhibitor p21 may exert its neuroprotective effects by inhibiting proteins involved in neuronal apoptosis cascades such as caspase 3 and pro death-stress –activated protein kinase (SAPK/JNK) (Langley et al., 2008).

While we did not observe an increase in CST neuron survival after application of NT3 or NT3+CNTF, the neurotrophins CNTF and NT3 have previously been shown to support the survival of corticospinal neurons grown in mixed cortical cultures *in vitro* (Giehl, K.M. 2001; Junger and Junger 1998). Differences in culture media composition or ages of cultured neurons, in this case P2 vs P8, may account for the difference in survival response by CST neurons in my hands. Furthermore, in the current study we used the nuclear stain DAPI to reveal pyknotic nuclei and nuclear fragments and these cells were deemed “dead” and excluded from quantification. Although DAPI has been used previously to label pyknotic nuclei (Diaz et al., 2000), perhaps using the viability stain PI or a fluorescent live/dead stain would reveal an acute neurotrophin-mediated trend for CST neuroprotection that is more similar to previous research.

4.2.2 HDAC inhibitor treatment increased the number of primary neurites and branch points exhibited by corticospinal neurons in vitro

TSA increased the number of primary neurites (Figure 3.6) and branch points (Figure 3.7) of transected CST neurons in culture. This increase occurred independent of

growth factor application. The branching behavior and number of primary neurites exhibited by terminally mature corticospinal neurons has not yet been assessed after application of HDAC inhibitors *in vitro*. The increase in branching and increased number of primary neurites observed in this study is consistent with changes in neuronal plasticity observed *in vivo* after injury (Onifer, Smith, and Fouad, 2011); it is tempting to speculate that HDAC inhibitor treatment may confer a heightened state of plasticity onto CST neurons, making them better able to regenerate after injury.

4.2.3 HDAC inhibitor treatment increased corticospinal neurite outgrowth *in vitro*

Both TSA and Tubastatin A were able to promote YFP-positive, corticospinal neurite outgrowth in the absence of NT3 and CNTF compared to the baseline condition (Figure 3.8). TSA also enhanced CST neurite outgrowth in the presence of NT3 compared to neurons treated with NT3 alone. After modifying our sampling and quantification paradigm, we found that in the presence of NT3+CNTF, TSA and Tubastatin A were also able to promote increased neurite outgrowth compared to neurons grown in the baseline and NT3+CNTF alone conditions. HDAC inhibitors can work alone or in conjunction with NT3+CNTF to promote neurite outgrowth of CST neurons. Although we were able to assess CST-specific outgrowth in response to HDAC inhibition, we are unable to say if HDAC inhibitor treatment directly affects neuronal outgrowth or if this phenomena is attributable to the effects HDAC inhibitors may be exerting on other cell types present in the mixed cortical culture. This will be addressed further in the future directions section.

While treatment with either TSA or Tubastatin A can promote neurite outgrowth of embryonic cortical neurons and cerebellar granular neurons (CGNs) *in vitro* (Gaub et al.,

2010; Riviuccio et al., 2009), this is the first study to illustrate the neurite outgrowth promoting effects of HDAC inhibitors on more mature corticospinal neurons *in vitro*. Little is understood about the specific mechanisms responsible for HDAC inhibitor-mediated neurite outgrowth. HDAC inhibitors can cause chromatin relaxation, which allows subsequent increase in transcription of previously silenced genes, so it is possible that HDAC inhibitors are effecting change in neurite outgrowth in a transcriptionally dependent manner. However, pan-HDAC inhibitors, like TSA, inhibit 11 HDACs, some of which are found in the cytoplasm as well as in the nucleus, to varying degrees. Furthermore, HDAC enzymes have also been shown to modify the function of non-histone targets including chaperone proteins, transcription factors and cytoskeletal proteins (Kazantsev and Thompson, 2008). It is therefore, possible that TSA might exert its neurite outgrowth promoting effects through both transcriptional dependent and independent means.

First, I will address the possibility that HDAC inhibitors promote outgrowth by altering transcription. The growth associated protein, GAP 43, has been shown to be important for neurite extension and growth cone dynamics and our lab has demonstrated previously that the expression of this protein is silenced in mature neurons by methylation and HDAC activity (Macdonald et al., 2010). This study directly implicates HDAC activity in the repression of neurite outgrowth associated genes in mature neurons. Recent research has demonstrated that TSA can promote the expression of GAP 43 and neurite outgrowth in a CGNs culture (Gaub et al., 2010). Interestingly, after TSA treatment the increased outgrowth and expression of GAP 43 was abolished when TSA was applied in concert with the transcriptional repressor Flavopiridol (Gaub et al., 2010). This suggests that the

observed hyperacetylation, increase in GAP43 expression and neurite growth were dependent on transcription (Gaub et al., 2010).

It is also possible that there could also be transcriptional independent mechanisms at work as TSA is a pan-HDAC inhibitor that hinders the activity of 11 HDAC isoforms, some of which have non-histone targets. HDAC 6, one of the isoforms inhibited by TSA, is predominantly cytosolic and can deacetylate cortactin and alpha tubulin (Kazantsev and Thompson, 2008; Riviuccio et al., 2009; Zhang et al., 2007). Cortactin has been implicated in neurite outgrowth and can be found in areas of dynamic actin assembly such as lamellipodia and neuronal growth cones (Du et al., 1998; Zhang et al., 2007). HDAC 6 can deacetylate cortactin, rendering it unable to interact with F-actin and resulting in impairments in the cytoskeletal rearrangements required for cell motility and possibly neurite extension (Lowery and Van Vactor, 2009; Zhang et al., 2007). Tubastatin A is an isoform specific inhibitor of HDAC 6, which can promote neurite outgrowth (Riviuccio et al., 2009). After Tubastatin A treatment, the expression level of acetylated alpha tubulin increased, but the level of H3 and H4 acetylation (two of the histones contained within the nucleosome) remained unchanged; this potentially implicates Tubastatin A in transcriptional independent mechanisms of promoting neurite outgrowth (Zhang et al., 2007).

HDAC 6 can also deacetylate alpha tubulin *in vitro* and *in vivo*, indicating that this isoform may play a role in regulating microtubule dynamics and consequently cell motility (Haggarty et al., 2003; Hubbert et al., 2002; Zhang et al., 2003). Acetylation of microtubules can increase their stability and the rate of anterograde flow, possibly resulting in growth cone progression (Bulinski, 2007).

Recently, HDAC 6 has been found to associate with Elongator, a multisubunit protein complex, which is primarily involved in transcript elongation but can also acetylate alpha tubulin (Creppe et al., 2009). Elongator is important for the regulation of dendritic and axonal outgrowth and dendritic branching of cortical projection neurons (Creppe et al., 2009). Neutralizing the catalytic activity of Elongator results in a reduction in the amount of alpha tubulin as well as a decrease in branching and axon extension in cortical projection neurons (Creppe et al., 2009).

Interestingly, both TSA and Tubastatin A increased neurite outgrowth of CST neurons in the current study and there is no significant difference in the neurite outgrowth observed between the two inhibitors. Although we cannot definitively conclude whether the effects on neurite outgrowth were transcriptionally dependent or independent, it is possible that CST neurons can increase neurite growth in response to treatment with HDAC inhibitors through both mechanisms.

Irrespective of the mechanisms involved, our findings illustrate that HDAC inhibitors can enhance neuron survival, branching and neurite outgrowth of more mature corticospinal neurons in vitro. This suggests that TSA and Tubastatin A could potentially serve as therapeutics for promoting regeneration of CST neurons that have been shown to be particularly refractory to regeneration after injury.

4.3 Future Directions

4.3.1 Establishing a purified population of CST neurons

In order to definitively say that HDAC inhibitors are exerting their effects directly on CST neurons and not indirectly through other cell types in the mixed culture, it would be

beneficial to treat a pure population of CST neurons with HDAC inhibitors and establish whether this produces the same increase in outgrowth. A more pure population of CST neurons could be established by FACS sorting cells harvested from the Thy1YFP16JRS mouse based on their YFP expression. Previous research has shown that cortical layer five neurons can be successfully purified using FACS after retrograde labeling using green fluorescent microspheres (Molyneaux et al., 2005). The FACS sorted cells survived and retained the typical molecular (Ctip2, Otx1 not Lmo4) as well as morphological characteristics (tufted apical and basal dendrites) of corticospinal neurons (Molyneaux et al., 2005). I have previously FACS sorted cells harvested from our P8 transgenic mouse and they have survived in the presence of astrocyte conditioned media and growth factors. Establishing a more pure population of CST neurons in this manner would be necessary to definitively test whether HDAC inhibitors are directly or indirectly affecting CST neuron outgrowth.

4.3.2 Determining which specific HDACs are expressed by CST neurons in vitro

In order to ascertain which specific HDAC enzymes are expressed by CST neurons *in vitro*, qPCR could be performed using HDAC isoform specific primers on FACS purified CST neurons. Knowledge of which HDACs are specifically expressed by CST neurons would allow the appropriate selection of isoform specific HDAC inhibitors, possibly reducing off target effects and potential toxicity present after pan-HDAC inhibition. After establishing a CST-specific HDAC expression profile it would be possible to perform a more directed investigation into how each of the implicated HDAC enzymes could be involved in regulating CST neurite outgrowth. Co-immunoprecipitation experiments could

be performed to establish the binding partners of the implicated HDAC isoforms. HDAC isoform specific inhibitor experiments could be performed in the presence of pathway inhibitors aimed at neutralizing intracellular signaling cascades known to be involved in CST neurite outgrowth like PI3K/Akt or MAPK/ERK. If the HDAC isoform of interest does not have a specific inhibitor siRNA knockdown of the specific HDAC isoform could be performed. A comparison of neurite outgrowth after either HDAC inhibitor treatment or HDAC inhibitor treatment in conjunction with a known pathway inhibitor (ie PI3K inhibitor LY 294002, or ERK inhibitor PD 98059) could shed light on whether or not the specific isoform is mediating neurite outgrowth effects through a certain intracellular signaling pathway.

4.3.3 Determining whether the desired inhibitor of interest is causing transcription of previously silenced genes

In order to establish whether or not HDAC inhibitor treatment of CST neurons is resulting in outgrowth due to the expression of previously silenced genes, a microarray could be performed on a control un-treated culture and a culture treated with an HDAC inhibitor. The comparison of these two data sets could potentially allow for the identification of growth promoting genes known to be involved in outgrowth that are up-regulated after treatment.

REFERENCES

- Arlotta, P., Molyneaux, B. J., Chen, J., Inoue, J., Kominami, R., and Macklis, J. D. (2005). Neuronal subtype-specific genes that control corticospinal motor neuron development in vivo. *Neuron* **45**(2), 207-21.
- Berry, M., Carlile, J., and Hunter, A. (1996). Peripheral nerve explants grafted into the vitreous body of the eye promote the regeneration of retinal ganglion cell axons severed in the optic nerve. *J Neurocytol* **25**(2), 147-70.
- Borisoff, J.F., Chan, C.C., Hiebert, G.W., Oschipok, L., Robertson, G.S., Zamboni, R., Steeves, J.D. and Tetzlaff, W. (2003). Suppression of Rho-kinase activity promotes axonal growth on inhibitory CNS substrates. *Mol Cell Neurosci* **22**(3), 405-16.
- Bradbury, E. J., Khemani, S., Von, R., King, Priestley, J. V., and McMahon, S. B. (1999). NT-3 promotes growth of lesioned adult rat sensory axons ascending in the dorsal columns of the spinal cord. *Eur J Neurosci* **11**(11), 3873-83.
- Cadotte, D. W., and Fehlings, M. G. (2011). Spinal cord injury: a systematic review of current treatment options. *Clin Orthop Relat Res* **469**(3), 732-41.
- Caroni, P., Savio, T., and Schwab, M. E. (1988). Central nervous system regeneration: oligodendrocytes and myelin as non-permissive substrates for neurite growth. *Prog Brain Res* **78**, 363-70.
- Cheney, P. D., Fetz, E. E., and Mewes, K. (1991). Neural mechanisms underlying corticospinal and rubrospinal control of limb movements. *Prog Brain Res* **87**, 213-52.
- Cohen, N. R., Taylor, J. S., Scott, L. B., Guillery, R. W., Soriano, P., and Furley, A. J. (1998). Errors in corticospinal axon guidance in mice lacking the neural cell adhesion molecule L1. *Curr Biol* **8**(1), 26-33.
- Dergham, P., Ellezam, B., Essagian, C., Avedissian, H., Lubell, W. D., and McKerracher, L. (2002). Rho signaling pathway targeted to promote spinal cord repair. *J Neurosci* **22**(15), 6570-7.
- Diaz, B., Serna, J., De Pablo, F., and de la Rosa, E. J. (2000). In vivo regulation of cell death by embryonic (pro)insulin and the insulin receptor during early retinal neurogenesis. *Development* **127**(8), 1641-9.
- Dokmanovic, M., and Marks, P. A. (2005). Prospects: histone deacetylase inhibitors. *J Cell Biochem* **96**(2), 293-304.

- Fawcett, J. W., and Asher, R. A. (1999). The glial scar and central nervous system repair. *Brain Res Bull* **49**(6), 377-91.
- Fetz, E. E. (1968). Pyramidal tract effects on interneurons in the cat lumbar dorsal horn. *J Neurophysiol* **31**(1), 69-80.
- Finger, J. H., Bronson, R. T., Harris, B., Johnson, K., Przyborski, S. A., and Ackerman, S. L. (2002). The netrin 1 receptors Unc5h3 and Dcc are necessary at multiple choice points for the guidance of corticospinal tract axons. *J Neurosci* **22**(23), 10346-56.
- Fishman, P. S., and Kelley, J. P. (1984). The fate of severed corticospinal axons. *Neurology* **34**(9), 1161-7.
- Fitch, M. T., and Silver, J. (1997). Activated macrophages and the blood-brain barrier: inflammation after CNS injury leads to increases in putative inhibitory molecules. *Exp Neurol* **148**(2), 587-603.
- Fitch, M. T., and Silver, J. (2008). CNS injury, glial scars, and inflammation: Inhibitory extracellular matrices and regeneration failure. *Exp Neurol* **209**(2), 294-301.
- Fournier, A. E., Takizawa, B. T., and Strittmatter, S. M. (2003). Rho kinase inhibition enhances axonal regeneration in the injured CNS. *J Neurosci* **23**(4), 1416-23.
- Gaub, P., Tedeschi, A., Puttagunta, R., Nguyen, T., Schmandke, A. and Di Giovanni, S. (2010). HDAC inhibition promotes neuronal outgrowth and counteracts growth cone collapse through CBP/p300 and P/CAF-dependent p53 acetylation. *Cell Death Differ* **17**(9), 1392-408.
- Gianino, S., Stein, S. A., Li, H., Lu, X., Biesiada, E., Ulas, J., and Xu, X. M. (1999). Postnatal growth of corticospinal axons in the spinal cord of developing mice. *Brain Res Dev Brain Res* **112**(2), 189-204.
- Giehl, K. M. (2001). Trophic dependencies of rodent corticospinal neurons. *Rev Neurosci* **12**(1), 79-94.
- Giehl, K. M., and Tetzlaff, W. (1996). BDNF and NT-3, but not NGF, prevent axotomy-induced death of rat corticospinal neurons in vivo. *Eur J Neurosci* **8**(6), 1167-75.
- Goldberg, J. L., Espinosa, J. S., Xu, Y., Davidson, N., Kovacs, G. T., and Barres, B. A. (2002). Retinal ganglion cells do not extend axons by default: promotion by neurotrophic signaling and electrical activity. *Neuron* **33**(5), 689-702.
- Grill, R., Murai, K., Blesch, A., Gage, F. H., and Tuszynski, M. H. (1997). Cellular delivery of neurotrophin-3 promotes corticospinal axonal growth and partial functional recovery after spinal cord injury. *J Neurosci* **17**(14), 5560-72.

- Guest, J. D., Hesse, D., Schnell, L., Schwab, M. E., Bunge, M. B., and Bunge, R. P. (1997). Influence of IN-1 antibody and acidic FGF-fibrin glue on the response of injured corticospinal tract axons to human Schwann cell grafts. *J Neurosci Res* **50**(5), 888-905.
- Guth, L., Barrett, C. P., Donati, E. J., Anderson, F. D., Smith, M. V., and Lifson, M. (1985). Essentiality of a specific cellular terrain for growth of axons into a spinal cord lesion. *Exp Neurol* **88**(1), 1-12.
- Haas, C. A., Rauch, U., Thon, N., Merten, T., and Deller, T. (1999). Entorhinal cortex lesion in adult rats induces the expression of the neuronal chondroitin sulfate proteoglycan neurocan in reactive astrocytes. *J Neurosci* **19**(22), 9953-63.
- Hill, C. E., Beattie, M. S., and Bresnahan, J. C. (2001). Degeneration and sprouting of identified descending supraspinal axons after contusive spinal cord injury in the rat. *Exp Neurol* **171**(1), 153-69.
- Hollis, E. R., 2nd, Jamshidi, P., Low, K., Blesch, A., and Tuszynski, M. H. (2009). Induction of corticospinal regeneration by lentiviral trkB-induced Erk activation. *Proc Natl Acad Sci U S A* **106**(17), 7215-20.
- Hsu, J. Y., Stein, S. A., and Xu, X. M. (2005). Temporal and spatial distribution of growth-associated molecules and astroglial cells in the rat corticospinal tract during development. *J Neurosci Res* **80**(3), 330-40.
- Huang, E. J., and Reichardt, L. F. (2003). Trk receptors: roles in neuronal signal transduction. *Annu Rev Biochem* **72**, 609-42.
- Hunt, D., Coffin, R. S., and Anderson, P. N. (2002). The Nogo receptor, its ligands and axonal regeneration in the spinal cord; a review. *J Neurocytol* **31**(2), 93-120.
- Iseda, T., Nishio, T., Kawaguchi, S., Kawasaki, T., and Wakisaka, S. (2003). Spontaneous regeneration of the corticospinal tract after transection in young rats: collagen type IV deposition and astrocytic scar in the lesion site are not the cause but the effect of failure of regeneration. *J Comp Neurol* **464**(3), 343-55.
- Iseda, T., Okuda, T., Kane-Goldsmith, N., Mathew, M., Ahmed, S., Chang, Y. W., Young, W., and Grumet, M. (2008). Single, high-dose intraspinal injection of chondroitinase reduces glycosaminoglycans in injured spinal cord and promotes corticospinal axonal regrowth after hemisection but not contusion. *J Neurotrauma* **25**(4), 334-49.
- Iwaniuk, A. N., Pellis, S. M., and Whishaw, I. Q. (1999). Is digital dexterity really related to corticospinal projections?: a re-analysis of the Heffner and Masterton data set using modern comparative statistics. *Behav Brain Res* **101**(2), 173-87.

- Johannessen, C. U. (2000). Mechanisms of action of valproate: a commentary. *Neurochem Int* **37**(2-3), 103-10.
- Joosten, E. A., and Bar, D. P. (1999). Axon guidance of outgrowing corticospinal fibres in the rat. *J Anat* **194** (Pt 1), 15-32.
- Junger, H., and Junger, W. G. (1998). CNTF and GDNF, but not NT-4, support corticospinal motor neuron growth via direct mechanisms. *Neuroreport* **9**(16), 3749-54.
- Kazantsev, A. G., and Thompson, L. M. (2008). Therapeutic application of histone deacetylase inhibitors for central nervous system disorders. *Nat Rev Drug Discov* **7**(10), 854-68.
- Kennedy, T. E., Serafini, T., de la Torre, J. R., and Tessier-Lavigne, M. (1994). Netrins are diffusible chemotropic factors for commissural axons in the embryonic spinal cord. *Cell* **78**(3), 425-35.
- Kouchi, Z., Igarashi, T., Shibayama, N., Inanobe, S., Sakurai, K., Yamaguchi, H., Fukuda, T., Yanagi, S., Nakamura, Y., and Fukami, K. (2011). Phospholipase Cdelta3 regulates RhoA/Rho kinase signaling and neurite outgrowth. *J Biol Chem* **286**(10), 8459-71.
- Kubasak, M. D., Jindrich, D. L., Zhong, H., Takeoka, A., McFarland, K. C., Munoz-Quiles, C., Roy, R. R., Edgerton, V. R., Ramon-Cueto, A., and Phelps, P. E. (2008). OEG implantation and step training enhance hindlimb-stepping ability in adult spinal transected rats. *Brain* **131**(Pt 1), 264-76.
- Lemon, R. N., and Griffiths, J. (2005). Comparing the function of the corticospinal system in different species: organizational differences for motor specialization? *Muscle Nerve* **32**(3), 261-79.
- Li, Y., and Raisman, G. (1995). Sprouts from cut corticospinal axons persist in the presence of astrocytic scarring in long-term lesions of the adult rat spinal cord. *Exp Neurol* **134**(1), 102-11.
- Lingor, P., Teusch, N., Schwarz, K., Mueller, R., Mack, H., Bahr, M., and Mueller, B. K. (2007). Inhibition of Rho kinase (ROCK) increases neurite outgrowth on chondroitin sulphate proteoglycan in vitro and axonal regeneration in the adult optic nerve in vivo. *J Neurochem* **103**(1), 181-9.
- Liu, K., Lu, Y., Lee, J. K., Samara, R., Willenberg, R., Sears-Kraxberger, I., Tedeschi, A., Park, K. K., Jin, D., Cai, B., Xu, B., Connolly, L., Steward, O., Zheng, B., and He, Z. (2010). PTEN deletion enhances the regenerative ability of adult corticospinal neurons. *Nat Neurosci* **13**(9), 1075-81.

- Looby, S., and Flanders, A. (2011). Spine trauma. *Radiol Clin North Am* **49**(1), 129-63.
- Lu, P., Blesch, A., and Tuszynski, M. H. (2001). Neurotrophism without neurotropism: BDNF promotes survival but not growth of lesioned corticospinal neurons. *J Comp Neurol* **436**(4), 456-70.
- MacDonald, J. L., and Roskams, A. J. (2008). Histone deacetylases 1 and 2 are expressed at distinct stages of neuro-glial development. *Dev Dyn* **237**(8), 2256-67.
- MacDonald, J. L. and Roskams, A. J.(2009). Epigenetic regulation of nervous system development by DNA methylation and histone deacetylation. *Prog Neurobiol* **88**(3), 170-83.
- MacDonald, J.L., Verster, A., Berndt, A. and Roskams, A. J. (2010). MBD2 and MeCP2 regulate distinct transitions in the stage-specific differentiation of olfactory receptor neurons. *Mol Cell Neurosci* **14**(1)55-67.
- McKerracher, L., and Higuchi, H. (2006). Targeting Rho to stimulate repair after spinal cord injury. *J Neurotrauma* **23**(3-4), 309-17.
- Metin, C., Deleglise, D., Serafini, T., Kennedy, T. E., and Tessier-Lavigne, M. (1997). A role for netrin-1 in the guidance of cortical efferents. *Development* **124**(24), 5063-74.
- Miller, M. W., Chiaia, N. L., and Rhoades, R. W. (1990). Intracellular recording and injection study of corticospinal neurons in the rat somatosensory cortex: effect of prenatal exposure to ethanol. *J Comp Neurol* **297**(1), 91-105.
- Molnar, Z., and Cheung, A. F. (2006). Towards the classification of subpopulations of layer V pyramidal projection neurons. *Neurosci Res* **55**(2), 105-15.
- Molyneaux, B. J., Arlotta, P., Hirata, T., Hibi, M., and Macklis, J. D. (2005). Fezl is required for the birth and specification of corticospinal motor neurons. *Neuron* **47**(6), 817-31.
- Monsul, N. T., Geisendorfer, A. R., Han, P. J., Banik, R., Pease, M. E., Skolasky, R. L., Jr., and Hoffman, P. N. (2004). Intraocular injection of dibutyryl cyclic AMP promotes axon regeneration in rat optic nerve. *Exp Neurol* **186**(2), 124-33.
- Morrison, B. E., Majdzadeh, N., and D'Mello, S. R. (2007). Histone deacetylases: focus on the nervous system. *Cell Mol Life Sci* **64**(17), 2258-69.
- Morrison, B. E., Majdzadeh, N., Zhang, X., Lyles, A., Bassel-Duby, R., Olson, E. N., and D'Mello, S. R. (2006). Neuroprotection by histone deacetylase-related protein. *Mol Cell Biol* **26**(9), 3550-64.

- Nash, M., Pribrig, H., Fournier, A. E., and Jacobson, C. (2009). Central nervous system regeneration inhibitors and their intracellular substrates. *Mol Neurobiol* **40**(3), 224-35.
- Ozdinler, P. H., and Macklis, J. D. (2006). IGF-I specifically enhances axon outgrowth of corticospinal motor neurons. *Nat Neurosci* **9**(11), 1371-81.
- Park, K. K., Liu, K., Hu, Y., Smith, P. D., Wang, C., Cai, B., Xu, B., Connolly, L., Kramvis, I., Sahin, M., and He, Z. (2008). Promoting axon regeneration in the adult CNS by modulation of the PTEN/mTOR pathway. *Science* **322**(5903), 963-6.
- Parr, A. M., Kulbatski, I., Zahir, T., Wang, X., Yue, C., Keating, A., and Tator, C. H. (2008). Transplanted adult spinal cord-derived neural stem/progenitor cells promote early functional recovery after rat spinal cord injury. *Neuroscience* **155**(3), 760-70.
- Ragancokova, D., Jahn, K., Kotsiari, A., Schlesinger, F., Haastert, K., Stangel, M., Petri, S., and Krampfl, K. (2009). Analysis of neuroprotective effects of valproic acid on primary motor neurons in monoculture or co-cultures with astrocytes or Schwann cells. *Cell Mol Neurobiol* **29**(6-7), 1037-43.
- Ramer, L. M., Au, E., Richter, M. W., Liu, J., Tetzlaff, W., and Roskams, A. J. (2004). Peripheral olfactory ensheathing cells reduce scar and cavity formation and promote regeneration after spinal cord injury. *J Comp Neurol* **473**(1), 1-15.
- Ramer, L. M., Ramer, M. S., and Steeves, J. D. (2005). Setting the stage for functional repair of spinal cord injuries: a cast of thousands. *Spinal Cord* **43**(3), 134-61.
- Ramon-Cueto, A., Cordero, M. I., Santos-Benito, F. F., and Avila, J. (2000). Functional recovery of paraplegic rats and motor axon regeneration in their spinal cords by olfactory ensheathing glia. *Neuron* **25**(2), 425-35.
- Richter, M. W., and Roskams, A. J. (2008). Olfactory ensheathing cell transplantation following spinal cord injury: hype or hope? *Exp Neurol* **209**(2), 353-67.
- Richter, M. W., and Roskams, A. J. (2009). Corticospinal neurons respond differentially to neurotrophins and myelin-associated glycoprotein in vitro. *J Neurosci Res* **87**(10), 2222-36.
- Rivieccio, M. A., Brochier, C., Willis, D. E., Walker, B. A., D'Annibale, M. A., McLaughlin, K., Siddiq, A., Kozikowski, A. P., Jaffrey, S. R., Twiss, J. L., Ratan, R. R., and Langley, B. (2009). HDAC6 is a target for protection and regeneration following injury in the nervous system. *Proc Natl Acad Sci U S A* **106**(46), 19599-604.
- Sato, Y., and Oohira, A. (2009). Chondroitin sulfate, a major niche substance of neural stem cells, and cell transplantation therapy of neurodegeneration combined with niche modification. *Curr Stem Cell Res Ther* **4**(3), 200-9.

- Schnell, L., Schneider, R., Kolbeck, R., Barde, Y. A., and Schwab, M. E. (1994). Neurotrophin-3 enhances sprouting of corticospinal tract during development and after adult spinal cord lesion. *Nature* **367**(6459), 170-3.
- Schnell, L., and Schwab, M. E. (1990). Axonal regeneration in the rat spinal cord produced by an antibody against myelin-associated neurite growth inhibitors. *Nature* **343**(6255), 269-72.
- Silver, J., and Miller, J. H. (2004). Regeneration beyond the glial scar. *Nat Rev Neurosci* **5**(2), 146-56.
- Southwood, C. M., Peppi, M., Dryden, S., Tainsky, M. A., and Gow, A. (2007). Microtubule deacetylases, SirT2 and HDAC6, in the nervous system. *Neurochem Res* **32**(2), 187-95.
- Suzuki, T. (2009). Explorative study on isoform-selective histone deacetylase inhibitors. *Chem Pharm Bull (Tokyo)* **57**(9), 897-906.
- Tedeschi, A., Nguyen, T., Puttagunta, R., Gaub, P., and Di Giovanni, S. (2009). A p53-CBP/p300 transcription module is required for GAP-43 expression, axon outgrowth, and regeneration. *Cell Death Differ* **16**(4), 543-54.
- Terashima, T. (1995). Anatomy, development and lesion-induced plasticity of rodent corticospinal tract. *Neurosci Res* **22**(2), 139-61.
- Tetzlaff, W., Alexander, S. W., Miller, F. D., and Bisby, M. A. (1991). Response of facial and rubrospinal neurons to axotomy: changes in mRNA expression for cytoskeletal proteins and GAP-43. *J Neurosci* **11**(8), 2528-44.
- Tetzlaff, W., Okon, E. B., Karimi-Abdolrezaee, S., Hill, C. E., Sparling, J. S., Plemel, J. R., Plunet, W. T., Tsai, E. C., Baptiste, D., Smithson, L. J., Kawaja, M. D., Fehlings, M. G., and Kwon, B. K. (2010). A Systematic Review of Cellular Transplantation Therapies for Spinal Cord Injury. *J Neurotrauma*.
- Tischler, A. S., and Greene, L. A. (1975). Nerve growth factor-induced process formation by cultured rat pheochromocytoma cells. *Nature* **258**(5533), 341-2.
- Tom, V. J., Steinmetz, M. P., Miller, J. H., Doller, C. M., and Silver, J. (2004). Studies on the development and behavior of the dystrophic growth cone, the hallmark of regeneration failure, in an in vitro model of the glial scar and after spinal cord injury. *J Neurosci* **24**(29), 6531-9.
- Topark-Ngarm, A., Golonzhka, O., Peterson, V. J., Barrett, B., Jr., Martinez, B., Crofoot, K., Filtz, T. M., and Leid, M. (2006). CTIP2 associates with the NuRD complex on the promoter of p57KIP2, a newly identified CTIP2 target gene. *J Biol Chem* **281**(43), 32272-83.

- Wang, Z., and Zhang, Q. (2009). Genome-wide identification and evolutionary analysis of the animal specific ETS transcription factor family. *Evol Bioinform Online* **5**, 119-31.
- Whishaw, I. Q., Pellis, S. M., Gorny, B., Kolb, B. and Tetzlaff, W. (1993). Proximal and distal impairments in rat forelimb use in reaching follow unilateral pyramidal tract lesions. *Behav Brain Res* **56**(1), 59-76.
- Weidner, N., Blesch, A., Grill, R. J., and Tuszynski, M. H. (1999). Nerve growth factor-hypersecreting Schwann cell grafts augment and guide spinal cord axonal growth and remyelinate central nervous system axons in a phenotypically appropriate manner that correlates with expression of L1. *J Comp Neurol* **413**(4), 495-506.
- Windle, W. F., and Chambers, W. W. (1950). Regeneration in the spinal cord of the cat and dog. *J Comp Neurol* **93**(2), 241-57.
- Zhang, Y., Li, N., Caron, C., Matthias, G., Hess, D., Khochbin, S., and Matthias, P. (2003). HDAC-6 interacts with and deacetylates tubulin and microtubules in vivo. *EMBO J* **22**(5), 1168-79.
- Zhang, Y., Ng, H. H., Erdjument-Bromage, H., Tempst, P., Bird, A., and Reinberg, D. (1999). Analysis of the NuRD subunits reveals a histone deacetylase core complex and a connection with DNA methylation. *Genes Dev* **13**(15), 1924-35.

APPENDICES

Appendix A.1 The Average Number of DAPI Positive Cells, Excluding Pyknotic Nuclei, Listed by Experiment

Condition	Experiment Code					Average	SEM
	I 94	I96	I97	I99	I100		
No GF	436.6667	658.5	721.3333	591.25	1266	734.75	141.0125
No GF + TSA		1078.5	867.6667	805	1699	1112.542	204.0502
No GF + Tubastatin A			742.6667	803.5	1384	976.7222	204.637
NT3	462.6667	724	361.3333	574.5		530.625	77.78009
NT3 + TSA	653.6667	1057.5	583	806		775.0417	105.021
NT3 + Tubastatin A			581	596	1529.333	902.1111	313.6502
NT3+CNTF		1004	713.3333	909		875.4444	85.5717
NT3+CNTF+TSA	575.6667	843		1090.667		836.4444	148.7082
NT3 + CNTF +Tubastatin A			906.3333	1086.667	1925	1306	313.8567

Appendix A.2 The Average Number of Excluded DAPI Positive Pyknotic Nuclei or Nuclear Fragments Listed by Experiment

Condition	Experiment Code						Average	SEM
	I 94	I96	I97	I99	I100			
No GF	2374	2324	3120	2189.25	2960.666667	2593.583333	186.5857005	
No GF + TSA		3244	2638	2033.25	3257.333333	2793.145833	291.5835246	
No GF + Tubastatin A			2579.666667	2447.75	2813	2613.472222	106.9114208	
NT3	2660	2730	1669.666667	1951		2252.666667	262.148071	
NT3 + TSA	3104	2633	1823.666667	2081.333333		2410.5	286.2359976	
NT3 + Tubastatin A			1861	1995	2981.666667	2279.222222	353.3563469	
NT3+CNTF		2079	1751.666667	1529.666667		1786.777778	159.5523433	
NT3+CNTF+TSA	2353	2290		2234.333333		2292.444444	34.27891837	
NT3 + CNTF +Tubastatin								
A			2457.333333	3207.666667	3426	3030.333333	293.3594255	

Appendix A.3 The Average Number of NST Positive Neurons Listed by Experiment

Condition	Experiment Code					Average	SEM
	I 94	I96	I97	I99	I100		
No GF	56.854	151.1587	186.3204	196.5167	269.658	172.1016	34.66814
No GF + TSA		252.5847	171.5377	200.5054	336.5719	240.2999	36.20665
No GF + Tubastatin A			155.7372	218.2507	280.7213	218.2364	36.12258
NT3	82.06164	209.1636	93.23604	184.7736		142.3087	32.02951
NT3 + TSA	108.7266	224.5601	126.8414	214.3423		168.6176	29.65426
NT3 + Tubastatin A			134.9663	176.4756	364.8989	225.4469	70.83201
NT3+CNTF		239.705	139.7658	179.2548		186.2419	29.09517
NT3+CNTF+TSA	88.17294	150.5177		224.5319		154.4075	39.45818
NT3 + CNTF +Tubastatin A			191.7499	314.9522	385.1444	297.2822	56.58994

Appendix A.4 Average Number of GFP Positive Cells Listed by Experiment

Condition	Experiment Code					Average	SEM
	I 94	I96	I97	I99	I100		
No GF	13.71133	36.54675	76.67773	82.70109	72.5418	56.43574	13.37942
No GF + TSA		77.92163	77.15726	102.5168	96.95627	88.63798	6.509361
No GF + Tubastatin A			69.2908	115.463	76.5352	87.09632	14.33708
NT3	23.4572	48.0736	36.33809	74.31158		45.54512	10.82646
NT3 + 10nM TSA	48.06629	73.179	50.81817	110.0459		70.52733	14.32275
NT3 + Tubastatin A			53.37453	75.8708	85.54071	71.59535	9.528752
NT3+CNTF		42.8708	53.64267	78.6588		58.39076	10.60068
NT3+CNTF +10nM TSA	37.91724	41.93925		139.4599		73.10547	33.23688
NT3 + CNTF +Tubastatin A			76.16221	150.7569	83.97813	103.6324	23.69808

Appendix A.5 Average Number of Primary Neurites per YFP Positive Neuron Listed by Experiment

Condition	Experiment Code					Average	SEM
	I94	I96	I97	I99	I100		
No GF	3	3.45	4.15	4.92	2.81	3.666	0.389224
No GF + TSA		3.95	6.07	5.24	3.75	4.7525	0.54943
No GF + Tubastatin A			4.17	4.62	4.2	4.33	0.145263
NT3	3.27	4.65	4.07	4.1		4.0225	0.284059
NT3 + TSA	4.93	4.35	4.82	4.28		4.595	0.163834
NT3 + Tubastatin A			3.81	4	3.96	3.923333	0.057833
NT3+CNTF		3.9	5.39	3.92		4.403333	0.493382
NT3 + CNTF +TSA	4.533	5.12		4		4.551	0.323451
NT3 + CNTF +Tubastatin A			4.75	4.16	4	4.303333	0.228066

Appendix A.6 Average Number of Branch Points per YFP Positive Neuron Listed by Experiment

Condition	Experiment Code					Average	SEM
	I94	I96	I97	I99	I100		
No GF	2.633333	9.4	5.26	8.04	6.15	6.296667	1.165928
No GF + TSA		10.75	9.64	8.88	10.13	9.85	0.395116
No GF + Tubastatin A			7.97	7.85	9.68	8.5	0.591717
NT3	3.466667	6.4	6.23	5.59		5.421667	0.674592
NT3 + TSA	5.4	11	9.25	6.48		8.0325	1.278954
NT3 + Tubastatin A			7.23	5.92	11.13	8.093333	1.564765
NT3+CNTF		8.45	9.93	7.58		8.653333	0.685983
NT3 + CNTF +TSA	7.5	14.18		7.13		9.603333	2.290892
NT3 + CNTF +Tubastatin A			8.75	8	11.33	9.36	1.008543

Appendix A.7 Average Length (μm) of Neurite Outgrowth per YFP Positive Neuron Listed by Experiment

Condition	Experiment Code					Average	SEM
	I94	I96	I97	I99	I100		
No GF	406	1430	645.01	1664	812	991.402	238.7146
No GF + TSA		3299	2062.85	4471	2223	3013.963	557.8561
No GF + Tubastatin A			1941.583	2105	1925	1990.528	57.43765
NT3	446	1700	915.53	1415		1119.133	276.8131
NT3 + TSA	1063.667	2907	1293.213	2533		1949.22	453.9357
NT3 + Tubastatin A			1488.573	2169	2410	2022.524	275.8994
NT3+CNTF		2730	2146.08	2243		2373.027	180.6715
NT3+CNTF+TSA	1359	8179		3344		4294	2025.315
NT3 + CNTF +Tubastatin A			2552.683	3138	4629	3439.894	618.1141

Appendix A.8 Average Length (μm) of YFP Positive Neurite Outgrowth per 20x Field of View Listed by Experiment

Condition	Experiment Code					Average	SEM
	I94	I96	I97	I99	I100		
No GF	250.82	1384	991	2136.8	1080.9	1168.704	305.4075
NT3+CNTF		1827	1355	2444		1875.333	315.304
NT3+CNTF+TSA	726.3333	3534.7		4256.6		2839.211	1076.828
NT3+CNTF+Tubastatin A			1921	4928	2859.7	3236.233	888.2537